A hybrid polynomial dimensional decomposition for uncertainty quantification of high-dimensional complex systems

Vaibhav Yadav^{1,*}, Sharif Rahman²

College of Engineering, The University of Iowa, Iowa City, Iowa 52242, U.S.A.

Abstract

This paper presents a novel hybrid polynomial dimensional decomposition (PDD) method for stochastic computing in high-dimensional complex systems. When a stochastic response does not possess a strongly additive or a strongly multiplicative structure alone, then the existing additive and multiplicative PDD methods may not provide a sufficiently accurate probabilistic solution of such a system. To circumvent this problem, a new hybrid PDD method was developed that is based on a linear combination of an additive and a multiplicative PDD approximation, a broad range of orthonormal polynomial bases for Fourier-polynomial expansions of component functions, and a dimension-reduction or sampling technique for estimating the expansion coefficients. Two numerical problems involving mathematical functions or uncertain dynamic systems were solved to study how and when a hybrid PDD is more accurate and efficient than the additive or multiplicative PDD. The results show that the univariate hybrid PDD method is slightly more expensive than the univariate additive or multiplicative PDD approximations, but it yields significantly more accurate stochastic solutions than the latter two methods. Therefore, the univariate truncation of the hybrid PDD is ideally suited to solving stochastic problems that may otherwise mandate expensive bivariate or higher-variate additive or multiplicative PDD approximations. Finally, a coupled acoustic-structural analysis of a pickup truck subjected to 46 random variables was performed, demonstrating the ability of the new method to solve large-scale engineering problems.

Keywords:

ANOVA, HDMR, dimension reduction, stochastic dynamics

1. Introduction

Polynomial dimensional decomposition (PDD) is a hierarchical and convergent expansion of a general, high-dimensional stochastic response function in terms of polynomial functions of input variables with increasing dimensions [1-4]. The decomposition ameliorates the curse of dimensionality [5] to some extent by developing an input-output behavior of complex systems with low effective dimensions [6], wherein the degrees of interactions between input variables attenuate rapidly or vanish altogether. However, the original PDD, referred to as the additive PDD (A-PDD) in this paper, constitutes a sum of lowerdimensional component functions and is, therefore, predicated on an additive nature of a multivariate function decomposition. In contrast, when a response function is of a multiplicative nature, suitable multiplicative-type decompositions, such as the factorized PDD (F-PDD) [7], should be explored. Nonetheless, A-PDD or F-PDD is relevant as long as the dimensional hierarchy of a stochastic response is also additive or multiplicative.

This paper presents a new hybrid PDD method for solving general high-dimensional stochastic problems commonly encountered in engineering and applied sciences. Section 2 provides a brief exposition of the existing additive and multiplicative PDD approximations, setting the stage for the new method developed. The hybrid PDD method, optimally blending A-PDD and F-PDD approximations, is described in Section 3 along with the second-moment properties of the resultant approximation. Section 4 focuses on the univariate hybrid approximation, resulting in explicit formulae for the hybrid

Unfortunately, the dimensional structure of a response function, in general, is not known a priori. Therefore, indiscriminately using A-PDD or F-PDD for general stochastic analysis is not desirable. Further complications may arise when a complex system exhibits a response that is dominantly neither additive nor multiplicative. In the latter case, hybrid approaches coupling both additive and multiplicative decompositions, preferably selected optimally, are needed. For such decompositions, it is unknown which truncation parameter should be selected when compared with that for A-PDD or F-PDD. More specifically, is it possible for the univariate truncation of a hybrid decomposition to produce stochastic solutions that are as good as or close to those obtained from higher-variate truncations of A-PDD or F-PDD? If the answer is yes, then a significant cost saving for high-dimensional uncertainty quantification is anticipated. That is the principal motivation of this work.

[☆]Grant sponsor: U.S. National Science Foundation; Grant Nos. CMMI-0653279, CMMI-1130147.

^{*}Corresponding author.

Email addresses: vaibhav-yadav@uiowa.edu (Vaibhav Yadav),

rahman@engineering.uiowa.edu (Sharif Rahman)

¹Adjunct Lecturer.

²Professor.

model parameters and second-moment statistics. The mean-squared error analyses pertaining to univariate A-PDD, F-PDD, and hybrid PDD approximations are also discussed. Section 5 explains dimension-reduction integration and the quasi Monte Carlo method for calculating the PDD expansion coefficients. Section 6 presents two numerical examples for illustrating the accuracy, efficiency, and convergence properties of the hybrid PDD method. In Section 7, a large, complex engineering problem, entailing coupled acoustic-structural analysis of a pickup truck, is solved using the hybrid PDD method. Finally, conclusions are drawn in Section 8.

2. Polynomial Dimensional Decomposition

Let \mathbb{N} , \mathbb{N}_0 , \mathbb{R} , and \mathbb{R}_0^+ represent the sets of positive integer (natural), non-negative integer, real, and non-negative real numbers, respectively. For $k \in \mathbb{N}$, denote by \mathbb{R}^k the k-dimensional Euclidean space, by \mathbb{N}_0^k the k-dimensional multi-index space, and by $\mathbb{R}^{k \times k}$ the set of $k \times k$ real-valued matrices. These standard notations will be used throughout the paper.

Let (Ω, \mathcal{F}, P) be a complete probability space, where Ω is a sample space, \mathcal{F} is a σ -field on Ω , and $P: \mathcal{F} \to [0,1]$ is a probability measure. With \mathcal{B}^N representing the Borel σ -field on \mathbb{R}^N , $N \in \mathbb{N}$, consider an \mathbb{R}^N -valued random vector $\mathbf{X} := (X_1, \cdots, X_N) : (\Omega, \mathcal{F}) \to (\mathbb{R}^N, \mathcal{B}^N)$, which describes the statistical uncertainties in all system and input parameters of a high-dimensional stochastic problem. The probability law of \mathbf{X} is completely defined by its joint probability density function $f_{\mathbf{X}}: \mathbb{R}^N \to \mathbb{R}^+_0$. Assuming independent coordinates of \mathbf{X} , its joint probability density $f_{\mathbf{X}}(\mathbf{x}) = \prod_{i=1}^{i=N} f_i(x_i)$ is expressed by a product of marginal probability density functions f_i of X_i , $i=1,\cdots,N$, defined on the probability triple $(\Omega_i,\mathcal{F}_i,P_i)$ with a bounded or an unbounded support on \mathbb{R} . For a given $u \subseteq \{1,\cdots,N\}$, $f_{\mathbf{X}_{-u}}(\mathbf{x}_{-u}) := \prod_{i=1,i\neq u}^N f_i(x_i)$ defines the marginal density function of $\mathbf{X}_{-u} := \mathbf{X}_{\{1,\cdots,N\}\setminus u}$.

Let $y(\mathbf{X}) := y(X_1, \dots, X_N)$, a real-valued, measurable transformation on (Ω, \mathcal{F}) , define a high-dimensional stochastic response of interest and $\mathcal{L}_2(\Omega, \mathcal{F}, P)$ represent a Hilbert space of square-integrable functions y with respect to the induced generic measure $f_{\mathbf{X}}(\mathbf{x})d\mathbf{x}$ supported on \mathbb{R}^N . The ANOVA dimensional decomposition (ADD), expressed by the recursive form [8–10]

$$y(\mathbf{X}) = \sum_{u \in \{1, \dots, N\}} y_u(\mathbf{X}_u),\tag{1}$$

$$y_{\emptyset} = \int_{\mathbb{R}^{N}} y(\mathbf{x}) f_{\mathbf{X}}(\mathbf{x}) d\mathbf{x}, \tag{2}$$

$$y_{u}(\mathbf{X}_{u}) = \int_{\mathbb{R}^{N-|u|}} y(\mathbf{X}_{u}, \mathbf{x}_{-u}) f_{\mathbf{X}_{-u}}(\mathbf{x}_{-u}) d\mathbf{x}_{-u} - \sum_{v \subset u} y_{v}(\mathbf{X}_{v}), \quad (3)$$

is a finite, hierarchical expansion in terms of its input variables with increasing dimensions, where $u \subseteq \{1, \dots, N\}$ is a subset with the complementary set $-u = \{1, \dots, N\} \setminus u$ and cardinality $0 \le |u| \le N$, and y_u is a |u|-variate component function describing a constant or the interactive effect of $\mathbf{X}_u = (X_{i_1}, \dots, X_{i_{|u|}})$, $1 \le i_1 < \dots < i_{|u|} \le N$, a subvector of \mathbf{X} , on y when |u| = 0 or |u| > 0. The summation in Equation (1) comprises 2^N terms,

with each term depending on a group of variables indexed by a particular subset of $\{1, \dots, N\}$, including the empty set \emptyset . In Equation (3), $(\mathbf{X}_u, \mathbf{x}_{-u})$ denotes an N-dimensional vector whose ith component is X_i if $i \in u$ and x_i if $i \notin u$. When $u = \emptyset$, the sum in Equation (3) vanishes, resulting in the expression of the constant function y_\emptyset in Equation (2). When $u = \{1, \dots, N\}$, the integration in Equation (3) is on the empty set, reproducing Equation (1) and hence finding the last function $y_{\{1,\dots,N\}}$. Indeed, all component functions of y can be obtained by interpreting literally Equation (3).

The ADD component functions y_u , $u \subseteq \{1, \dots, N\}$, are uniquely determined from the annihilating conditions [8–10],

$$\int_{\mathbb{R}} y_u(\mathbf{x}_u) f_i(x_i) dx_i = 0 \text{ for } i \in u,$$
(4)

resulting in two remarkable properties: (1) the component functions, y_u , $\emptyset \neq u \subseteq \{1, \dots, N\}$, have zero means; and (2) two distinct component functions y_u and y_v , where $u \subseteq \{1, \dots, N\}$, $v \subseteq \{1, \dots, N\}$, and $u \neq v$, are orthogonal [10]. However, the ADD component functions are difficult to obtain because they require calculation of high-dimensional integrals.

2.1. Additive PDD

Let $\{\psi_{ij}(X_i);\ j=0,1,\cdots\}$ be a set of orthonormal polynomial basis functions in the Hilbert space $\mathcal{L}_2(\Omega_i,\mathcal{F}_i,P_i)$ that is consistent with the probability measure P_i of X_i . For a given $\emptyset\neq u=\{i_1,\cdots,i_{|u|}\}\subseteq \{1,\cdots,N\},\ 1\leq |u|\leq N,\ 1\leq i_1<\cdots< i_{|u|}\leq N,\ \text{denote a product probability triple by }(\mathsf{x}_{p=1}^{p=|u|}\Omega_{i_p},\mathsf{x}_{p=1}^{p=|u|}\mathcal{F}_{i_p},\mathsf{x}_{p=1}^{p=|u|}P_{i_p}),\ \text{and the associated space of square integrable }|u|$ -variate component functions of y by $\mathcal{L}_2(\mathsf{x}_{p=1}^{p=|u|}\Omega_{i_p},\mathsf{x}_{p=1}^{p=|u|}\mathcal{F}_{i_p},\mathsf{x}_{p=1}^{p=|u|}P_{i_p}):=\{y_u:\int_{\mathbb{R}^{|u|}}y_u^2(\mathbf{x}_u)f_{\mathbf{X}_u}(\mathbf{x}_u)d\mathbf{x}_u<\infty\},\ \text{which is a Hilbert space.}$ Since the joint density of $(X_{i_1},\cdots,X_{i_{|u|}})$ is separable (independence), i.e., $f_{\mathbf{X}_u}(\mathbf{x}_u)=\prod_{p=1}^{|u|}f_{i_p}(x_{i_p}),\ \text{the product polynomial }\psi_{u\mathbf{j}_{|u|}}(\mathbf{X}_u):=\prod_{p=1}^{|u|}\psi_{i_pj_p}(X_{i_p}),\ \text{where }\mathbf{j}_{|u|}=(j_1,\cdots,j_{|u|})\in\mathbb{N}_0^{|u|},\ \text{a }|u|\text{-dimensional multi-index with }\infty\text{-norm }\|\mathbf{j}_{|u|}\|_{\infty}:=\max(j_1,\cdots,j_{|u|}),\ \text{constitutes an orthonormal basis in }\mathcal{L}_2(\mathsf{x}_{p=1}^{p=|u|}\Omega_{i_p},\mathsf{x}_{p=1}^{p=|u|}\mathcal{F}_{i_p},\mathsf{x}_{p=1}^{p=|u|}P_{i_p}).\ \text{Two important properties of these product polynomials from the tensor product of Hilbert spaces are as follows.}$

Proposition 1. The product polynomials $\psi_{u\mathbf{j}_{|u|}}(\mathbf{X}_u)$, $\emptyset \neq u \subseteq \{1, \dots, N\}$ have zero means, that is,

$$\mathbb{E}\left[\psi_{u\mathbf{j}_{|u|}}(\mathbf{X}_{u})\right] = 0. \tag{5}$$

Proposition 2. Two distinct product polynomials $\psi_{u\mathbf{j}_{|u|}}(\mathbf{X}_u)$ and $\psi_{v\mathbf{k}_{|v|}}(\mathbf{X}_v)$, where $\emptyset \neq u \subseteq \{1, \dots, N\}$, $\emptyset \neq v \subseteq \{1, \dots, N\}$, $j_1, \dots, j_{|u|} \neq 0$, $k_1, \dots, k_{|v|} \neq 0$, are uncorrelated and each has unit variance, that is,

$$\mathbb{E}\left[\psi_{u\mathbf{j}_{|u|}}(\mathbf{X}_u)\psi_{v\mathbf{k}_{|v|}}(\mathbf{X}_v)\right] = \begin{cases} 1 & \text{if } u = v; \ \mathbf{j}_{|u|} = \mathbf{k}_{|v|}, \\ 0 & \text{otherwise.} \end{cases}$$
 (6)

From the standard Hilbert space theory, every non-constant component function $y_u \in \mathcal{L}_2(\times_{p=1}^{p=|u|}\Omega_{i_p},\times_{p=1}^{p=|u|}\mathcal{F}_{i_p},\times_{p=1}^{p=|u|}P_{i_p})$ of y

can be expanded as [1, 2]

$$y_{u}(\mathbf{X}_{u}) = \sum_{\substack{\mathbf{j}_{|u|} \in \mathbb{N}_{0}^{|u|} \\ j_{1}, \cdots, j_{|u|} \neq 0}} C_{u\mathbf{j}_{|u|}} \psi_{u\mathbf{j}_{|u|}}(\mathbf{X}_{u}), \ \emptyset \neq u \subseteq \{1, \cdots, N\}, \quad (7)$$

with

$$C_{u\mathbf{j}_{|u|}} := \int_{\mathbb{R}^{N}} y(\mathbf{x}) \psi_{u\mathbf{j}_{|u|}}(\mathbf{x}_{u}) f_{\mathbf{X}}(\mathbf{x}) d\mathbf{x}, \ \emptyset \neq u \subseteq \{1, \cdots, N\}, \ \mathbf{j}_{|u|} \in \mathbb{N}_{0}^{|u|}, \ (8)$$

representing the corresponding expansion coefficient. Note that the summation in Equation (7) precludes $j_1, \dots, j_{|u|} = 0$, that is, the individual degree of each variable X_i in $\psi_{uj_{|u|}}$, $i \in u$ cannot be *zero* since y_u is a strictly |u|-variate function and has a *zero* mean. The end result of combining Equations (1) and (7) is the A-PDD [1, 2],

$$y(\mathbf{X}) = y_0 + \sum_{\substack{\emptyset \neq u \subseteq \{1, \dots, N\} \\ j_1, \dots, j_{|u|} \neq 0}} \sum_{\mathbf{j}_{|u|} \in \mathbb{N}_0^{|u|}} C_{u\mathbf{j}_{|u|}} \psi_{u\mathbf{j}_{|u|}}(\mathbf{X}_u), \tag{9}$$

providing an exact, hierarchical expansion of y in terms of an infinite number of coefficients or orthonormal polynomials. Using Propositions 1 and 2, all component functions y_u , $\emptyset \neq u \subseteq \{1, \dots, N\}$ in Equation (7) are found to satisfy the annihilating conditions of the ADD. Therefore, A-PDD can be viewed as the polynomial version of ADD and is, therefore, endowed with all desirable properties of ADD.

In many physical and engineering applications, the function y can be approximated by a sum of at most S-variate component functions, where $1 \le S \le N$, resulting in the S-variate, mth-order A-PDD approximation

$$\tilde{y}_{S,m}(\mathbf{X}) = y_{\emptyset} + \sum_{\substack{\emptyset \neq u \subseteq \{1, \dots, N\}\\1 \leq |u| \leq S}} \sum_{\mathbf{j}_{|u|} \in \mathbb{N}_{0}^{|u|}, ||\mathbf{j}_{|u|}||_{\infty} \leq m} C_{u\mathbf{j}_{|u|}} \psi_{u\mathbf{j}_{|u|}}(\mathbf{X}_{u}), \quad (10)$$

containing $\sum_{k=0}^{S} \binom{N}{S-k} m^{S-k}$ number of A-PDD coefficients and corresponding orthonormal polynomials. Due to its additive structure, the approximation in Equation (10) includes degrees of interaction among at most S input variables $X_{i_1}, \cdots, X_{i_S}, 1 \leq i_1 \leq \cdots \leq i_S \leq N$. For instance, by selecting S=1 and S, the functions, S, and S, respectively, provide univariate and bivariate S, and should not be viewed as first- and second-order approximations, nor do they limit the nonlinearity of S. Depending on how the component functions are constructed, arbitrarily high-order univariate and bivariate terms of S could be lurking inside S, and S, when S in the mean-square sense, permitting Equation (10) to generate a hierarchical and convergent sequence of approximations of S.

Applying the expectation operator on $\tilde{y}_{S,m}(\mathbf{X})$ and $(\tilde{y}_{S,m}(\mathbf{X}) - y_{\emptyset})^2$ and noting Propositions 1 and 2, the mean [11]

$$\mathbb{E}\left[\tilde{y}_{S,m}(\mathbf{X})\right] = y_{\emptyset} \tag{11}$$

of the *S*-variate, *m*th-order A-PDD approximation matches the exact mean $\mathbb{E}[y(\mathbf{X})]$, regardless of *S* or *m*, and the approximate

variance [11]

$$\tilde{\sigma}_{S,m}^{2} := \mathbb{E}\left[\left(\tilde{y}_{S,m}(\mathbf{X}) - \mathbb{E}\left[\tilde{y}_{S,m}(\mathbf{X})\right]\right)^{2}\right]$$

$$= \sum_{\substack{\emptyset \neq u \subseteq \{1,\cdots,N\}\\1 \leq |u| \leq S}} \sum_{\substack{\mathbf{j}_{|u|} \in \mathbb{N}_{0}^{|u|}, ||\mathbf{j}_{|u|}||_{\infty} \leq m\\j_{1},\cdots,j_{|u|} \neq 0}} C_{u\mathbf{j}_{|u|}}^{2}$$

$$(12)$$

is calculated as the sum of squares of the expansion coefficients from the S-variate, mth-order A-PDD approximation of $y(\mathbf{X})$. It is elementary to show that the approximate variance in Equation (12) approaches the exact variance of y when $S \to N$ and $m \to \infty$ [11]. The mean-square convergence of $\tilde{y}_{S,m}$ is guaranteed as y, and its component functions are all members of the associated Hilbert spaces.

For the special case of S = 1, the univariate A-PDD approximation

$$\tilde{y}_{1,m}(\mathbf{X}) = y_0 + \sum_{i=1}^{N} \sum_{i=1}^{m} C_{ij} \psi_{ij}(X_i)$$
(13)

of y(X) yields the exact mean

$$\mathbb{E}\left[\tilde{y}_{1,m}(\mathbf{X})\right] = y_{\emptyset},\tag{14}$$

and an approximate variance

$$\tilde{\sigma}_{1,m}^2 := \mathbb{E}\left[\left(\tilde{\mathbf{y}}_{1,m}(\mathbf{X}) - \mathbb{E}\left[\tilde{\mathbf{y}}_{1,m}(\mathbf{X})\right]\right)^2\right] = \sum_{i=1}^N \sum_{i=1}^m C_{ij}^2$$
(15)

that depends on $m < \infty$.

2.2. Factorized PDD

The factorized dimensional decomposition of the multivariate function

$$y(\mathbf{X}) = \prod_{u \subseteq \{1, \dots, N\}} [1 + z_u(\mathbf{X}_u)], \tag{16}$$

where z_u , $u \subseteq \{1, \dots, N\}$ are various component functions of input variables with increasing dimensions. Like the sum in Equation (1), the product in Equation (16) comprises 2^N terms, with each term depending on a group of variables indexed by a particular subset of $\{1, \dots, N\}$, including the empty set \emptyset . This multiplicative decomposition exists and is unique for any square-integrable function $y \in \mathcal{L}_2(\Omega, \mathcal{F}, P)$ with a non-zero mean. Tunga and Demiralp [12] originally proposed this decomposition, calling it factorized high-dimensional model representation. Subsequently, Yadav and Rahman [7], and Rahman [13] derived a recursive relationship between the component functions of ANOVA and factorized dimensional decompositions, as described by Theorem 1, leading to F-PDD.

Theorem 1. The recursive relationships between component functions of the ANOVA and factorized dimensional decompositions of a non-zero mean, square-integrable function $y : \mathbb{R}^N \to \mathbb{R}$, represented by Equations (1) and (16), respectively, are

$$1 + z_u(\mathbf{X}_u) = \frac{\sum_{v \subseteq u} y_v(\mathbf{X}_v)}{\prod_{v \subset u} [1 + z_v(\mathbf{X}_v)]}, \ u \subseteq \{1, \dots, N\}.$$
 (17)

Proof. See Theorem 8 of Yadav and Rahman [7] or Theorem 3.4 of Rahman [13]. \Box

Applying Equation (7) into Equation (17) and then combining with Equation (16) forms the F-PDD of

$$y(\mathbf{X}) = y_{\emptyset} \prod_{\emptyset \neq u \subseteq \{1, \dots, N\}} \left[\frac{y_{\emptyset} + \sum_{\emptyset \neq v \subseteq u} \sum_{\substack{\mathbf{j}_{[v]} \in \mathbb{N}_{0}^{[v]} \\ j_{1}, \dots, j_{[v]} \neq 0}}{C_{v\mathbf{j}_{[v]}} \psi_{v\mathbf{j}_{[v]}}(\mathbf{X}_{v})} \right]$$

$$= \sum_{\emptyset \neq u \subseteq \{1, \dots, N\}} \left[\frac{\sum_{\emptyset \neq v \subseteq u} \sum_{\substack{\mathbf{j}_{[v]} \in \mathbb{N}_{0}^{[v]} \\ j_{1}, \dots, j_{[v]} \neq 0}}{C_{v\mathbf{j}_{[v]}} \psi_{v\mathbf{j}_{[v]}}(\mathbf{X}_{v})} \right]$$
(18)

as an exact representation of $y(\mathbf{X})$, where infinite orthonormal polynomials of increasing dimensions are structured with a multiplicative hierarchy, as opposed to the additive hierarchy in Equation (9). Consequently, an S-variate, mth-order F-PDD approximation, retaining at most S-variate component functions and mth-order orthogonal polynomials, becomes

$$\hat{y}_{S,m}(\mathbf{X}) = y_{\emptyset} \prod_{\substack{\emptyset \neq u \subseteq \{1, \dots, N\}\\1 \leq |u| \leq S}} \left[\frac{y_{\emptyset} + \sum_{\emptyset \neq \nu \subseteq u} \sum_{\mathbf{j}_{|\nu|} \in \mathbb{N}_{0}^{|\nu|}, ||\mathbf{j}_{|u|}||_{\infty} \leq m} C_{\nu \mathbf{j}_{|\nu|}} \psi_{\nu \mathbf{j}_{|\nu|}} (\mathbf{X}_{\nu})}{\prod_{\nu \subset u} [1 + z_{\nu}(\mathbf{X}_{\nu})]} \right].$$

$$(19)$$

It is elementary to show that the S-variate, mth-order F-PDD approximation converges to $y(\mathbf{X})$ in the mean-square sense when $S \to N$ and $m \to \infty$.

Unlike Equations (11) and (12), the mean and variance of $\hat{y}_{S,m}(\mathbf{X})$, respectively defined as

$$\mathbb{E}\left[\hat{y}_{S,m}(\mathbf{X})\right] := \int_{\mathbb{R}^N} \hat{y}_{S,m}(\mathbf{x}) f_{\mathbf{X}}(\mathbf{x}) d\mathbf{x}$$
 (20)

and

$$\hat{\sigma}_{S,m}^{2} := \mathbb{E}\left[\left(\hat{y}_{S,m}(\mathbf{X}) - \mathbb{E}\left[\hat{y}_{S,m}(\mathbf{X})\right]\right)^{2}\right]$$
$$:= \int_{\mathbb{R}^{N}} \left(\hat{y}_{S,m}(\mathbf{x}) - \mathbb{E}\left[\hat{y}_{S,m}(\mathbf{X})\right]\right)^{2} f_{\mathbf{X}}(\mathbf{x}) d\mathbf{x}, \qquad (21)$$

do not produce closed-form or analytic expressions in terms of y_{\emptyset} and $C_{u\mathbf{j}_{|u|}}$ if S is selected arbitrarily. This is a drawback of F-PDD when compared with A-PDD. Having said so, they are easily estimated by sampling methods, such as quasi and crude Monte Carlo simulations (MCS), or even numerical integration if N is not overly large.

When S = 1, the univariate F-PDD approximation,

$$\hat{y}_{1,m}(\mathbf{X}) = y_{\emptyset} \left[\prod_{i=1}^{N} \left\{ 1 + \frac{1}{y_{\emptyset}} \sum_{j=1}^{m} C_{ij} \psi_{ij}(X_{i}) \right\} \right], \tag{22}$$

forms a product of univariate polynomials. Equation (22) results in the exact mean

$$\mathbb{E}\left[\hat{\mathbf{y}}_{1,m}(\mathbf{X})\right] = \mathbf{y}_{\emptyset},\tag{23}$$

and an approximate variance

$$\hat{\sigma}_{1,m}^{2} := \mathbb{E}\left[(\hat{y}_{1,m}(\mathbf{X}) - \mathbb{E}\left[\hat{y}_{1,m}(\mathbf{X}) \right])^{2} \right]$$

$$= y_{0}^{2} \left[\prod_{i=1}^{N} \left(1 + \frac{1}{y_{0}^{2}} \sum_{i=1}^{m} C_{ij}^{2} \right) - 1 \right]$$
(24)

that are valid for an arbitrary $m < \infty$.

3. Hybrid PDD

When a desired stochastic response exhibits neither a dominantly additive nor a dominantly multiplicative nature, then a mixed approach that optimally combines A-PDD and F-PDD approximations is needed. Two linear hybrid approximations are proposed.

3.1. Hybrid Approximations

Given S-variate, mth-order additive PDD and factorized PDD approximations $\tilde{y}_{S,m}(\mathbf{X})$ and $\hat{y}_{S,m}(\mathbf{X})$, let

$$\tilde{\mathbf{y}}_{S,m}\left(\mathbf{X}; \alpha_{S,m}, \beta_{S,m}, \ldots\right) := \begin{cases}
y_{0} & \text{if } S = 0, \\
h\left(\tilde{\mathbf{y}}_{S,m}\left(\mathbf{X}\right), \hat{\mathbf{y}}_{S,m}\left(\mathbf{X}\right); \alpha_{S,m}, \beta_{S,m}, \ldots\right) & \text{if } 1 \leq S < N, \\
y\left(\mathbf{X}\right) & \text{if } S = N, \ m \to \infty,
\end{cases}$$
(25)

define a general, S-variate, mth-order hybrid PDD approximation of y(X), where h is a chosen model function such that $\mathbb{E}\left[\bar{y}_{S,m}\left(\mathbf{X};\alpha_{S,m},\beta_{S,m},\ldots\right)\right]=y_{\emptyset}$ and $\alpha_{S,m},\beta_{S,m},\ldots$ are the associated model parameters. Define the *zero*-mean functions

$$w\left(\mathbf{X}\right) := y\left(\mathbf{X}\right) - y_{\emptyset},\tag{26}$$

$$\tilde{w}_{S,m}(\mathbf{X}) := \tilde{y}_{S,m}(\mathbf{X}) - y_{\emptyset}, \tag{27}$$

$$\hat{w}_{Sm}(\mathbf{X}) := \hat{y}_{Sm}(\mathbf{X}) - \mathbb{E}\left[\hat{y}_{Sm}(\mathbf{X})\right],\tag{28}$$

and

$$\bar{w}_{S,m}\left(\mathbf{X};\alpha_{S,m},\beta_{S,m},\ldots\right) := \bar{y}_{S,m}\left(\mathbf{X};\alpha_{S,m},\beta_{S,m},\ldots\right) - y_{\emptyset}, (29)$$

that will be used throughout this section. Theorem 2 and Corollary 1 describe two optimal linear hybrid approximations $\bar{y}_{S,m}(\mathbf{X};\alpha_{S,m},\beta_{S,m})$ and $\bar{y}'_{S,m}(\mathbf{X};\alpha'_{S,m},\beta'_{S,m})$ for $1 \leq S < N$, $m < \infty$, both producing the exact mean y_{\emptyset} . The two hybrid approximations have their *zero*-mean counterparts defined as

$$\bar{w}_{S,m}(\mathbf{X};\alpha_{S,m},\beta_{S,m}) := \bar{y}_{S,m}(\mathbf{X};\alpha_{S,m},\beta_{S,m}) - y_{\emptyset}$$
(30)

and

$$\bar{w}'_{S,m}\left(\mathbf{X};\alpha'_{S,m}\right) := \bar{y}'_{S,m}\left(\mathbf{X};\alpha'_{S,m}\right) - y_{\emptyset}.$$
(31)

Theorem 2. Given integers $1 \leq S < N < \infty$ and $1 \leq m < \infty$, let $\tilde{w}_{S,m}(\mathbf{X})$ and $\hat{w}_{S,m}(\mathbf{X})$ represent zero-mean, S-variate, mth-order additive PDD and factorized PDD approximations with variances $\tilde{\sigma}_{S,m}^2 := \mathbb{E}\left[\tilde{y}_{S,m}(\mathbf{X}) - y_0\right]^2 = \mathbb{E}\left[\tilde{w}_{S,m}^2(\mathbf{X})\right]$ and $\hat{\sigma}_{S,m}^2 := \mathbb{E}\left[\hat{y}_{S,m}(\mathbf{X}) - y_0\right]^2 = \mathbb{E}\left[\hat{w}_{S,m}^2(\mathbf{X})\right]$, respectively, of a

real-valued, zero-mean, square-integrable function $w(\mathbf{X})$. Then there exists an optimal, linear, S-variate, mth-order hybrid PDD approximation

$$\bar{w}_{S,m}(\mathbf{X};\alpha_{S,m},\beta_{S,m}) = \alpha_{S,m}\tilde{w}_{S,m}(\mathbf{X}) + \beta_{S,m}\hat{w}_{S,m}(\mathbf{X})$$
(32)

of w (X), where

$$\frac{\alpha_{S,m} = \frac{\partial^2 S,m}{\partial \alpha'_{S,m}} = 0. \qquad (41)}{\frac{\hat{\sigma}_{S,m}^2 \mathbb{E}\left[w(\mathbf{X})\,\tilde{w}_{S,m}(\mathbf{X})\right] - \mathbb{E}\left[\tilde{w}_{S,m}(\mathbf{X})\,\hat{w}_{S,m}(\mathbf{X})\right]\mathbb{E}\left[w(\mathbf{X})\,\hat{w}_{S,m}(\mathbf{X})\right]}{\left(33\right)}}, \text{ Again, swapping the orders of differential and expectation operators, and substituting the expression of } \tilde{w}'_{S,m}(\mathbf{X};\alpha'_{S,m}) \text{ from } Equation (38) results in the expression of } \alpha'_{S,m}(\mathbf{X};\alpha'_{S,m}) \text{ from } \mathbf{X}_{S,m}(\mathbf{X};\alpha'_{S,m}) = 0.$$

$$\beta_{S,m} = \frac{\tilde{\sigma}_{S,m}^{2} \mathbb{E}\left[w\left(\mathbf{X}\right) \hat{w}_{S,m}\left(\mathbf{X}\right)\right] - \mathbb{E}\left[\tilde{w}_{S,m}\left(\mathbf{X}\right) \hat{w}_{S,m}\left(\mathbf{X}\right)\right] \mathbb{E}\left[w\left(\mathbf{X}\right) \tilde{w}_{S,m}\left(\mathbf{X}\right)\right]}{\tilde{\sigma}_{S,m}^{2} \hat{\sigma}_{S,m}^{2} - \left(\mathbb{E}\left[\tilde{w}_{S,m}\left(\mathbf{X}\right) \hat{w}_{S,m}\left(\mathbf{X}\right)\right]\right)^{2}}$$
(34)

Proof. For a square-integrable function $w(\mathbf{X})$, define a secondmoment error

$$\bar{e}_{S,m} := \mathbb{E} \left[w \left(\mathbf{X} \right) - \bar{w}_{S,m} \left(\mathbf{X}; \alpha_{S,m}, \beta_{S,m} \right) \right]^2 \tag{35}$$

committed by its S-variate, mth-order hybrid PDD approximation $\bar{w}_{S,m}(\mathbf{X};\alpha_{S,m},\beta_{S,m})$. For $\bar{e}_{S,m}$ to be minimum, set

$$\frac{\partial \bar{e}_{S,m}}{\partial \alpha_{S,m}} = 0,
\frac{\partial \bar{e}_{S,m}}{\partial \beta_{S,m}} = 0.$$
(36)

Exchanging the orders of differential and expectation operators and substituting the expression of $\bar{w}_{S,m}(\mathbf{X}; \alpha_{S,m}, \beta_{S,m})$ from

$$\alpha_{S,m}\mathbb{E}\left[\tilde{w}_{S,m}^{2}\left(\mathbf{X}\right)\right] + \beta_{S,m}\mathbb{E}\left[\tilde{w}_{S,m}\left(\mathbf{X}\right)\hat{w}_{S,m}\left(\mathbf{X}\right)\right] = \mathbb{E}\left[w\left(\mathbf{X}\right)\tilde{w}_{S,m}\left(\mathbf{X}\right)\right], \alpha_{S,m}\mathbb{E}\left[\tilde{w}_{S,m}\left(\mathbf{X}\right)\hat{w}_{S,m}\left(\mathbf{X}\right)\right] + \beta_{S,m}\mathbb{E}\left[\hat{w}_{S,m}^{2}\left(\mathbf{X}\right)\right] = \mathbb{E}\left[w\left(\mathbf{X}\right)\hat{w}_{S,m}\left(\mathbf{X}\right)\right].$$

$$(37)$$

Noting $\tilde{\sigma}_{S,m}^2 = \mathbb{E}\left[\tilde{w}_{S,m}^2(\mathbf{X})\right]$ and $\hat{\sigma}_{S,m}^2 = \mathbb{E}\left[\hat{w}_{S,m}^2(\mathbf{X})\right]$, the solution Equations (37) produces the expressions of $\alpha_{S,m}$ and $\beta_{S,m}$ as in Equations (33) and (34), proving the theorem.

Corollary 1. Constraining the sum of two model parameters to be unity in Equation (32) through (37) creates another optimal, linear, S-variate hybrid approximation

$$\bar{w}'_{S,m}\left(\mathbf{X};\alpha'_{S,m}\right) = \alpha'_{S,m}\tilde{w}_{S,m}\left(\mathbf{X}\right) + \left(1 - \alpha'_{S,m}\right)\hat{w}_{S,m}\left(\mathbf{X}\right) \quad (38)$$

of w(X), $1 \le S < N < \infty$, $m < \infty$, where the optimal model parameter

$$\alpha_{S,m}' = \frac{\mathbb{E}\left[\left\{w\left(\mathbf{X}\right) - \hat{w}_{S,m}\left(\mathbf{X}\right)\right\} \left\{\tilde{w}_{S,m}\left(\mathbf{X}\right) - \hat{w}_{S,m}\left(\mathbf{X}\right)\right\}\right]}{\mathbb{E}\left[\tilde{w}_{S,m}\left(\mathbf{X}\right) - \hat{w}_{S,m}\left(\mathbf{X}\right)\right]^{2}}.$$
 (39)

Proof. For a square-integrable function $w(\mathbf{X})$, define another second-moment error

$$\bar{e}'_{S,m} := \mathbb{E}\left[w\left(\mathbf{X}\right) - \bar{w}'_{S,m}\left(\mathbf{X}; \alpha'_{S,m}\right)\right]^{2} \tag{40}$$

owing to its S-variate, mth-order hybrid PDD approximation $\bar{w}'_{S,m}(\mathbf{X};\alpha'_{S,m})$. For $\bar{e}'_{S,m}$ to be minimum, set

$$\frac{\partial \bar{e}'_{S,m}}{\partial \alpha'_{S,m}} = 0. \tag{41}$$

erators, and substituting the expression of $\bar{w}'_{S,m}(\mathbf{X}; \alpha'_{S,m})$ from Equation (38) results in the expression of $\alpha'_{S,m}$ as in Equation (39), proving the corollary.

Remark 1. The second hybrid approximation $\bar{w}'_{S,m}$ for S=1or 2 presented in Corollary 1 coincides with that proposed by Tunga and Demiralp [12]. However, the first hybrid approximation $\bar{w}_{S,m}$ – that is, Theorem 2 – is new. Furthermore, the two approximations, $\bar{w}_{S,m}$ and $\bar{w}'_{S,m}$, are not the same for a general truncation $2 \le S < N$. See a recent work of Rahman [13] for distinction between these two linear models, including a nonlinear variant, not discussed in this paper for brevity.

Remark 2. The hybrid PDD approximations exist for any function y or w with a finite variance. The approximations, $\bar{w}_{S,m}(\mathbf{X};\alpha_{S,m},\beta_{S,m})$ and $\bar{w}'_{S,m}(\mathbf{X};\alpha'_{S,m})$, for a given $1 \leq S <$ $N < \infty$, and $1 \le m < \infty$, can exactly reproduce the original zero-mean function $w(\mathbf{X})$ under the following two conditions: (1) If the original function is endowed with a purely additive structure, i.e., $w(\mathbf{X}) = \tilde{w}_{S,m}(\mathbf{X})$, then Equations (33), (34), and (39) yield $\alpha_{S,m} = \alpha'_{S,m} = 1$, and $\beta_{S,m} = 0$, which in turn results in $\bar{w}_{S,m}(\mathbf{X}) = \bar{w}'_{S,m}(\mathbf{X}) = \tilde{w}_{S,m}(\mathbf{X}) = w(\mathbf{X})$; (2) If the original function possesses a purely multiplicative structure, i.e., $w(\mathbf{X}) = \hat{w}_{S,m}(\mathbf{X})$, then Equations (33), (34), and (39) produce $\alpha_{S,m} = \alpha'_{S,m} = 0$ and $\beta_{S,m} = 1$, and therefore $\bar{w}_{S,m}(\mathbf{X}) = \bar{w}'_{S,m}(\mathbf{X}) = \hat{w}_{S,m}(\mathbf{X}) = w(\mathbf{X})$.

3.2. Second-moment properties

Applying the expectation operator on Equations (32) and (38) yields the exact mean

$$\mathbb{E}\left[\bar{y}_{S,m}\left(\mathbf{X};\alpha_{S,m},\beta_{S,m}\right)\right] = \mathbb{E}\left[\bar{y}'_{S,m}\left(\mathbf{X};\alpha'_{S,m}\right)\right] = y_{\emptyset},\tag{42}$$

by both the hybrid approximations. However, their respective variances, obtained by applying the expectation operator on $\bar{w}_{S,m}(\mathbf{X}; \alpha_{S,m}, \beta_{S,m})^2$ and $\bar{w}'_{S,m}(\mathbf{X}; \alpha'_{S,m}, \beta'_{S,m})^2$, respectively, vary according to

$$\bar{\sigma}_{S,m}^{2} := \mathbb{E}\left[\bar{w}_{S,m}^{2}(\mathbf{X}; \alpha_{S,m}, \beta_{S,m})\right]$$

$$= \alpha_{S,m}^{2} \tilde{\sigma}_{S,m}^{2} + \beta_{S,m}^{2} \hat{\sigma}_{S,m}^{2}$$

$$+2\alpha_{S,m}\beta_{S,m}\mathbb{E}\left[\tilde{w}_{S,m}(\mathbf{X})\hat{w}_{S,m}(\mathbf{X})\right]$$
(43)

and

$$\bar{\sigma}_{S,m}^{\prime 2} := \mathbb{E}\left[\bar{w}_{S,m}^{\prime 2}\left(\mathbf{X}; \alpha_{S,m}^{\prime}\right)\right]
= \alpha_{S,m}^{\prime 2} \tilde{\sigma}_{S,m}^{2} + \left(1 - \alpha_{S,m}^{\prime}\right)^{2} \hat{\sigma}_{S,m}^{2}
+ 2\alpha_{S,m}^{\prime} \left(1 - \alpha_{S,m}^{\prime}\right) \mathbb{E}\left[\tilde{w}_{S,m}\left(\mathbf{X}\right)\hat{w}_{S,m}\left(\mathbf{X}\right)\right]. (44)$$

Compared with the additive and factorized PDD approximations, the hybrid PDD approximations proposed require expectation of product of $\tilde{w}_{S,m}(\mathbf{X})$ and $\hat{w}_{S,m}(\mathbf{X})$ to calculate the variance

4. Univariate Hybrid PDD Approximation

At the root of developing the PDD methods lies the principal motive of achieving high accuracy in calculating the probabilistic characteristics of high-dimensional random responses while keeping the computational efforts to a minimum. This objective was attained through foresaking the inefficient higher-variate expansions and applying only univariate hybrid PDD approximations in solving high-dimensional stochastic problems. Considering the key advantage of high efficiency of a univariate additive [1] and factorized PDD [7] approximations, only the univariate hybrid PDD method was implemented in this work. Proposition 3 formally describes the univariate hybrid PDD approximation.

Proposition 3. A linear, univariate, mth-order hybrid PDD approximation of $w(\mathbf{X})$, obtained by setting S=1 in Equations (32)-(34), is

$$\bar{w}_{1,m}(\mathbf{X};\alpha_{1,m},\beta_{1,m}) = \alpha_{1,m}\tilde{w}_{1,m}(\mathbf{X}) + \beta_{1,m}\hat{w}_{1,m}(\mathbf{X})$$
(45)

where the model parameters

$$\alpha_{1,m} = \frac{\hat{\sigma}_{1,m}^2 - \mathbb{E}\left[w\left(\mathbf{X}\right)\hat{w}_{1,m}\left(\mathbf{X}\right)\right]}{\hat{\sigma}_{1,m}^2 - \tilde{\sigma}_{1,m}^2} \tag{46}$$

and

$$\beta_{1,m} = \frac{\mathbb{E}\left[w\left(\mathbf{X}\right)\hat{w}_{1,m}\left(\mathbf{X}\right)\right] - \tilde{\sigma}_{1,m}^{2}}{\hat{\sigma}_{1,m}^{2} - \tilde{\sigma}_{1,m}^{2}}.$$
(47)

Proof. Consider the univariate, *m*th-order additive and factorized PDD approximations,

$$\tilde{w}_{1,m}(\mathbf{X}) = \sum_{i=1}^{N} \sum_{i=1}^{m} C_{ij} \psi_{ij}(X_i), \tag{48}$$

$$\hat{w}_{1,m}(\mathbf{X}) = y_{\emptyset} \left[\prod_{i=1}^{N} \left\{ 1 + \frac{1}{y_{\emptyset}} \sum_{j=1}^{m} C_{ij} \psi_{ij}(X_{i}) \right\} \right] - y_{\emptyset}, \tag{49}$$

of

$$w\left(\mathbf{X}\right) = \sum_{\substack{\emptyset \neq u \subseteq \{1, \dots, N\}}} \sum_{\substack{\mathbf{j}_{|u|} \in \mathbb{N}_{0}^{|u|} \\ j_{1}, \dots, j_{|u|} \neq 0}} C_{u\mathbf{j}_{|u|}} \psi_{u\mathbf{j}_{|u|}}(\mathbf{X}_{u}). \tag{50}$$

From Propositions 1 and 2,

$$\mathbb{E}\left[w\left(\mathbf{X}\right)\tilde{w}_{1,m}\left(\mathbf{X}\right)\right] = \mathbb{E}\left[\tilde{w}_{1,m}\left(\mathbf{X}\right)\hat{w}_{1,m}\left(\mathbf{X}\right)\right]$$
$$= \sum_{i=1}^{N} \sum_{j=1}^{m} C_{ij}^{2} = \tilde{\sigma}_{1,m}^{2}. \tag{51}$$

Applying Equation (51) to Equations (33) and (34), the model parameters for S=1 and $m<\infty$ are obtained as in Equations (46) and (47).

Remark 3. The two parameters $\alpha_{1,m}$ and $\beta_{1,m}$ of the hybrid model described by Equation (45) add up to one. This is due to special properties of $\tilde{w}_{1,m}(\mathbf{X})$ and $\hat{w}_{1,m}(\mathbf{X})$ expressed in Equations (48) and (49). Therefore, the hybrid model described by Equation (38) at univariate truncation (S = 1) is redundant, as it leads to the same solution of the first model described by Equation (45).

Since $\beta_{1,m} = 1 - \alpha_{1,m}$, let

$$\bar{w}_{1,m}\left(\mathbf{X};\alpha_{1,m}\right) := \bar{y}_{1,m}\left(\mathbf{X};\alpha_{1,m}\right) - y_{\emptyset}$$

$$= \alpha_{1,m}\tilde{w}_{1,m}\left(\mathbf{X}\right) + \left(1 - \alpha_{1,m}\right)\hat{w}_{1,m}\left(\mathbf{X}\right) \quad (52)$$

denote the univariate hybrid PDD approximation of $w(\mathbf{X})$. The mean of $\bar{w}_{1,m}(\mathbf{X}; \alpha_{1,m})$ is *zero* and, therefore, $\mathbb{E}\left[\bar{y}_{1,m}(\mathbf{X}; \alpha_{1,m})\right] = y_{\emptyset}$, matching the exact mean of $y(\mathbf{X})$. The variance of $\bar{w}_{1,m}(\mathbf{X}; \alpha_{1,m})$ or $\bar{y}_{1,m}(\mathbf{X}; \alpha_{1,m})$ is

$$\bar{\sigma}_{1,m}^{2} := \mathbb{E}\left[\bar{w}_{1,m}^{2}(\mathbf{X}; \alpha_{1,m})\right]
= \left(2\alpha_{1,m} - \alpha_{1,m}^{2}\right)\tilde{\sigma}_{1,m}^{2} + \left(1 - \alpha_{1,m}\right)^{2}\hat{\sigma}_{1,m}^{2},$$
(53)

which is a linear combination of the variances from univariate additive PDD and univariate factorized PDD approximations. The variances $\tilde{\sigma}_{1,m}^2$ and $\hat{\sigma}_{1,m}^2$, expressed by Equations (15) and (24), are obtained from the univariate PDD expansion coefficients. However, determining the model parameter $\alpha_{1,m}$ involves evaluation of an N-dimensional integral that will incur additional computational expense in excess of the computations performed for estimating the PDD expansions coefficients. A quasi MCS was employed for estimating the model parameters, described as follows.

4.1. Calculation of the hybrid model parameter

The basic idea of a quasi MCS is to replace the random or pseudo-random samples in crude MCS by well-chosen deterministic samples that are highly equidistributed [14]. The qausi MCS samples are often selected from a low-discrepancy sequence [14–17] or by lattice rules [18] to minimize the integration errors. The estimation of the expectation of the multivariate function $w(\mathbf{X}) \hat{w}_{1,m}(\mathbf{X})$, which is a high-dimensional integral, comprises three simple steps: (1) generate a low-discrepancy point set $\mathcal{P}_L := \{\mathbf{u}^{(k)} \in [0,1]^N, \ k=1,\cdots,L\}$ of size $L \in \mathbb{N}$; (2) map each sample from \mathcal{P}_L to the sample $\mathbf{x}^{(k)} \in \mathbb{R}^N$ following the probability measure of the random input \mathbf{X} ; and (3) approximate the expectation as $\mathbb{E}\left[w(\mathbf{X}) \hat{w}_{1,m}(\mathbf{X})\right] \cong \frac{1}{L} \sum_{k=1}^{L} \left[w\left(\mathbf{x}^{(k)}\right) \hat{w}_{1,m}\left(\mathbf{x}^{(k)}\right)\right]$. Thus, using quasi MCS, the model parameter is given by

$$\alpha_{1,m} \cong \frac{\hat{\sigma}_{1,m}^2 - \frac{1}{L} \sum_{k=1}^{L} \left[w \left(\mathbf{x}^{(k)} \right) \hat{w}_{1,m} \left(\mathbf{x}^{(k)} \right) \right]}{\hat{\sigma}_{1,m}^2 - \tilde{\sigma}_{1,m}^2}, \tag{54}$$

where $\hat{\sigma}_{1,m}^2$ and $\tilde{\sigma}_{1,m}^2$ are obtained from Equations (15) and (24). However, when $\hat{\sigma}_{1,m}^2 = \mathbb{E}\left[\hat{w}_{1,m}^2(\mathbf{X})\right]$ and $\tilde{\sigma}_{1,m}^2 = \mathbb{E}\left[\tilde{w}_{1,m}^2(\mathbf{X})\right]$

are also estimated from a quasi MCS method, then the model parameter can also be obtained from

$$\alpha_{1,m} \cong \frac{\frac{1}{L} \sum_{k=1}^{L} \left[\hat{w}_{1,m}^{2} \left(\mathbf{x}^{(k)} \right) \right] - \frac{1}{L} \sum_{k=1}^{L} \left[w \left(\mathbf{x}^{(k)} \right) \hat{w}_{1,m} \left(\mathbf{x}^{(k)} \right) \right]}{\frac{1}{L} \sum_{k=1}^{L} \left[\hat{w}_{1,m}^{2} \left(\mathbf{x}^{(k)} \right) \right] - \frac{1}{L} \sum_{k=1}^{L} \left[\tilde{w}_{1,m}^{2} \left(\mathbf{x}^{(k)} \right) \right]}.$$
(55)

The well-known Koksma–Hlawka inequality reveals that the error committed by a quasi MCS is bounded by the variation of the integrand in the sense of Hardy and Krause and the star-discrepancy, a measure of uniformity, of the point set \mathcal{P}_L [14]. Therefore, constructing a point set with star-discrepancy as small as possible and seeking variance reduction of the integrand are vital for the success of the quasi MCS. It should be mentioned here that many authors, including Halton [15], Faure [16], Niederreiter [14], Sobol [17], and Wang [19], have extensively studied how to generate the best low-discrepancy point sets and sequences and to engender variance reduction. For a bounded variation of the integrand, the quasi MCS has a theoretical error bound $O(L^{-1}(\log L)^N)$ compared with the probabilistic error bound $O(N^{-1/2})$ of crude MCS, indicating significantly faster convergence of the quasi MCS than crude MCS.

Both Equations (54) and (55) were employed for estimating $\alpha_{1,m}$ in this work. Further details, clarifying which equation is used, are given in the Numerical Examples section.

4.2. Error analysis

Given the univariate truncation (S = 1), which approximation stemming from additive PDD, factorized PDD, and hybrid PDD is more accurate? Lemma 1 and Theorem 3 address this question.

Lemma 1. Given an integer $1 \le m < \infty$, the variance of the univariate factorized PDD approximation $\hat{y}_{1,m}(\mathbf{X})$ is greater than or equal to the variance of the univariate additive PDD approximation $\tilde{y}_{1,m}(\mathbf{X})$, that is,

$$\hat{\sigma}_{1,m}^2 \geq \tilde{\sigma}_{1,m}^2.$$

Proof. From Equation (24),

$$\hat{\sigma}_{1,m}^{2} = y_{\emptyset}^{2} \left[\prod_{i=1}^{N} \left(1 + \frac{1}{y_{\emptyset}^{2}} \sum_{j=1}^{m} C_{ij}^{2} \right) - 1 \right]$$

$$= \sum_{i=1}^{N} \sum_{j=1}^{m} C_{ij}^{2} + y_{\emptyset}^{2} \sum_{s=2}^{N} \sum_{\emptyset \neq u \subseteq \{1, \dots, N\}} \prod_{i \in u} \frac{1}{y_{\emptyset}^{2}} \sum_{j=1}^{m} C_{ij}^{2}$$

$$\geq \tilde{\sigma}_{1,m}^{2}, \qquad (56)$$

where the last line follows from Equation (15) and the recognition that the second term of the second line is non-negative. \Box

Theorem 3. Let $y(\mathbf{X})$ be a real-valued, square-integrable function with $\tilde{y}_{1,m}(\mathbf{X})$, $\hat{y}_{1,m}(\mathbf{X})$, and $\bar{y}_{1,m}(\mathbf{X})$ denoting its univariate additive PDD, univariate factorized PDD, and univariate hybrid PDD approximations, respectively, with $\tilde{\sigma}_{1,m}^2$, $\hat{\sigma}_{1,m}^2$, and

 $\bar{\sigma}_{1,m}^2$ as the variances obtained from respective approximations. If

$$\tilde{e}_{1,m} := \mathbb{E}\left[y\left(\mathbf{X}\right) - \tilde{y}_{1,m}\left(\mathbf{X}\right)\right]^{2} = \mathbb{E}\left[w\left(\mathbf{X}\right) - \tilde{w}_{1,m}\left(\mathbf{X}\right)\right]^{2}, (57)$$

$$\hat{e}_{1,m} := \mathbb{E} \left[y(\mathbf{X}) - \hat{y}_{1,m}(\mathbf{X}) \right]^2 = \mathbb{E} \left[w(\mathbf{X}) - \hat{w}_{1,m}(\mathbf{X}) \right]^2, (58)$$

and

$$\bar{e}_{1,m} := \mathbb{E}\left[y\left(\mathbf{X}\right) - \bar{y}_{1,m}\left(\mathbf{X}\right)\right]^2 = \mathbb{E}\left[w\left(\mathbf{X}\right) - \bar{w}_{1,m}\left(\mathbf{X}\right)\right]^2 \quad (59)$$

are the mean-squared errors committed by univariate additive PDD, univariate factorized PDD, and univariate hybrid PDD, respectively, in calculating σ^2 , the variance of $y(\mathbf{X})$, then,

$$\bar{e}_{1,m} \leq \tilde{e}_{1,m}$$

and

$$\bar{e}_{1,m} \leq \hat{e}_{1,m}$$
.

Proof. From Equations (57) and (59),

$$\tilde{e}_{1,m} = \sigma^2 - \tilde{\sigma}_{1,m}^2 \tag{60}$$

and

$$\bar{e}_{1,m} = \mathbb{E}\left[w^2(\mathbf{X})\right] + \mathbb{E}\left[\bar{w}^2(\mathbf{X})\right] - 2\mathbb{E}\left[w(\mathbf{X})\,\bar{w}_{1,m}(\mathbf{X})\right]$$
$$= \sigma^2 + \bar{\sigma}_{1\,m}^2 - 2\mathbb{E}\left[w(\mathbf{X})\,\bar{w}_{1,m}(\mathbf{X})\right]. \tag{61}$$

Subtracting Equation (60) from Equation (61) yields

$$\bar{e}_{1,m} - \tilde{e}_{1,m} = \bar{\sigma}_{1,m}^{2} - 2\mathbb{E}\left[w\left(\mathbf{X}\right)\bar{w}_{1,m}\left(\mathbf{X}\right)\right] + \tilde{\sigma}_{1,m}^{2} \\
= \left(2\alpha_{1,m} - \alpha_{1,m}^{2}\right)\tilde{\sigma}_{1,m}^{2} + \left(1 - \alpha_{1,m}\right)^{2}\hat{\sigma}_{1,m}^{2} + \tilde{\sigma}_{1,m}^{2} \\
-2\mathbb{E}\left[w\left(\mathbf{X}\right)\left\{\alpha_{1,m}\tilde{w}_{1,m}\left(\mathbf{X}\right) + \left(1 - \alpha_{1,m}\right)\hat{w}_{1,m}\left(\mathbf{X}\right)\right\}\right] \\
= 2\left(1 - \alpha_{1,m}\right)\left(\tilde{\sigma}_{1,m}^{2} - \mathbb{E}\left[w\left(\mathbf{X}\right)\hat{w}_{1,m}\left(\mathbf{X}\right)\right]\right) \\
+ \left(1 - \alpha_{1,m}\right)^{2}\left(\hat{\sigma}_{1,m}^{2} - \tilde{\sigma}_{1,m}^{2}\right) \\
= -\left(1 - \alpha_{1,m}\right)^{2}\left(\hat{\sigma}_{1,m}^{2} - \tilde{\sigma}_{1,m}^{2}\right) \\
\leq 0, \tag{62}$$

following Lemma 1, where the second equality uses Equations (53) and (52) and the last equality uses Equation (47).

Similarly, from Equation (58),

$$\hat{e}_{1,m} = \sigma^2 + \hat{\sigma}_{1,m}^2 - 2\mathbb{E}\left[w(\mathbf{X})\,\hat{w}_{1,m}(\mathbf{X})\right]. \tag{63}$$

Subtracting Equation (63) from Equation (61) yields

$$\begin{split} \bar{e}_{1,m} - \hat{e}_{1,m} &= \bar{\sigma}_{1,m}^2 - 2\mathbb{E}\left[w\left(\mathbf{X}\right)\bar{w}_{1,m}\left(\mathbf{X}\right)\right] - \hat{\sigma}_{1,m}^2 \\ &+ 2\mathbb{E}\left[w\left(\mathbf{X}\right)\hat{w}_{1,m}\left(\mathbf{X}\right)\right] \\ &= \left(2\alpha_{1,m} - \alpha_{1,m}^2\right)\tilde{\sigma}_{1,m}^2 + \left(1 - \alpha_{1,m}\right)^2\hat{\sigma}_{1,m}^2 \\ &- 2\mathbb{E}\left[w\left(\mathbf{X}\right)\left\{\alpha_{1,m}\tilde{w}_{1,m}\left(\mathbf{X}\right) + \left(1 - \alpha_{1,m}\right)\hat{w}_{1,m}\left(\mathbf{X}\right)\right\}\right] \\ &- \hat{\sigma}_{1,m}^2 + 2\mathbb{E}\left[w\left(\mathbf{X}\right)\hat{w}_{1,m}\left(\mathbf{X}\right)\right] \\ &= \tilde{\sigma}_{1,m}^2 - \hat{\sigma}_{1,m}^2 - 2\alpha_{1,m}\left(\tilde{\sigma}_{1,m}^2 - \mathbb{E}\left[w\left(\mathbf{X}\right)\hat{w}_{1,m}\left(\mathbf{X}\right)\right]\right) \\ &+ \left(1 - \alpha_{1,m}\right)^2\left(\hat{\sigma}_{1,m}^2 - \tilde{\sigma}_{1,m}^2\right) \\ &= -\alpha_{1,m}^2\left(\hat{\sigma}_{1,m}^2 - \tilde{\sigma}_{1,m}^2\right) \\ &\leq 0, \end{split}$$
(64)

following Lemma 1, where, again, the second equality uses Equations (53) and (52) and the last equality uses Equation (47).

The significance of Theorem 3 lies in providing analytical relations comparing the errors committed in calculating the variances by the univariate additive PDD, factorized PDD, and hybrid PDD approximations. It is clear from Theorem 3 that the error committed by univariate hybrid PDD can never be greater than the error committed by either univariate additive PDD or univariate factorized PDD.

5. Expansion Coefficients

The determination of the expansion coefficients, y_{\emptyset} and $C_{uj_{\|u\|}}$ in Equations (2) and (8), respectively, involves various N-dimensional integrals over \mathbb{R}^N . For large N, a full numerical integration employing an N-dimensional tensor product of a univariate quadrature formula is computationally prohibitive. Instead, a dimension-reduction Gaussian-integration scheme and a sampling technique were applied to estimate the coefficients efficiently.

5.1. Dimension-Reduction Integration

The dimension-reduction integration, developed by Xu and Rahman [20], entails approximating a high-dimensional integral of interest by a finite sum of lower-dimensional integrations. For calculating the expansion coefficients y_0 and $C_{uj_{[u]}}$, this is accomplished by replacing the *N*-variate function *y* in Equations (2) and (8) with an *R*-variate RDD approximation at a chosen reference point, where $R \leq N$ [10, 21]. The result is a reduced integration scheme, requiring evaluations of at most *R*-dimensional integrals.

Let $\mathbf{c} = (c_1, \dots, c_N) \in \mathbb{R}^N$ be a reference point of \mathbf{X} and $y(\mathbf{x}_v, \mathbf{c}_{-v})$ represent a |v|-variate component function of $y(\mathbf{x}), v \subseteq \{1, \dots, N\}$. Replacing $y(\mathbf{x})$ with an R-variate truncation of its referential dimensional decomposition [10, 21], the coefficients y_{\emptyset} and $C_{u\mathbf{j}_{|u|}}$ are estimated from [20]

$$y_{\emptyset} \cong \sum_{k=0}^{R} (-1)^{k} \binom{N-R+k-1}{k} \sum_{\substack{\nu \subseteq \{1,\cdots,N\}\\ |\nu|=R-k}} \int_{\mathbb{R}^{|\nu|}} y(\mathbf{x}_{\nu}, \mathbf{c}_{-\nu}) f_{\mathbf{X}_{\nu}}(\mathbf{x}_{\nu}) d\mathbf{x}_{\nu}$$

$$\tag{65}$$

and

$$C_{u\mathbf{j}_{|u|}} \cong \sum_{k=0}^{R} (-1)^{k} \binom{N-R+k-1}{k}$$

$$\times \sum_{\substack{v \subseteq \{1,\cdots,N\}\\|v|=R-k}} \int_{\mathbb{R}^{|v|}} y(\mathbf{x}_{v}, \mathbf{c}_{-v}) \psi_{u\mathbf{j}_{|u|}}(\mathbf{x}_{u}) f_{\mathbf{X}_{v}}(\mathbf{x}_{v}) d\mathbf{x}_{v}, \quad (66)$$

respectively, requiring evaluation of at most R-dimensional integrals. The reduced integration facilitates calculation of the coefficients approaching their exact values as $R \to N$, and is significantly more efficient than performing one N-dimensional integration, particularly when $R \ll N$. Hence, the computational

effort is significantly decreased using the dimension-reduction integration. For instance, when R=1 or 2, Equations (65) and (66) involve one-, or at most, two-dimensional integrations, respectively.

For a general function y, numerical integrations are still required for performing various |v|-dimensional integrals over $\mathbb{R}^{|v|}$, $0 \leq |v| \leq R$, in Equations (65) and (66). When R > 1, multivariate numerical integrations are conducted by constructing a tensor product of underlying univariate quadrature rules. For a given $v \subseteq \{1, \cdots, N\}$, $1 < |v| \leq R$, let $v = \{i_1, \cdots i_{|v|}\}$, where $1 \leq i_1 < \cdots < i_{|v|} \leq N$. Denote by $\{x_{i_p}^{(1)}, \cdots, x_{i_p}^{(n)}\} \subset \mathbb{R}$ a set of integration points of x_{i_p} and by $\{w_{i_p}^{(1)}, \cdots, w_{i_p}^{(n)}\}$ the associated weights generated from a chosen univariate quadrature rule and a positive integer $n \in \mathbb{N}$. Denote by $P^{(n)} = \times_{p=1}^{p=|v|} \{x_{i_p}^{(1)}, \cdots, x_{i_p}^{(n)}\}$ a rectangular grid consisting of all integration points generated by the variables indexed by the elements of v. Then the coefficients using dimension-reduction integration and numerical quadrature are approximated by

$$y_{\emptyset} \cong \sum_{i=0}^{R} (-1)^{i} \binom{N-R+i-1}{i} \sum_{\substack{v \subseteq \{1, \dots, N\} \\ |v|=R-i}} \sum_{\mathbf{k}_{|v|} \in P^{(n)}} w^{(\mathbf{k}_{|v|})} y(\mathbf{x}_{v}^{(\mathbf{k}_{|v|})}, \mathbf{c}_{-v})$$
(67)

and

$$C_{u\mathbf{j}_{|u|}} \cong \sum_{i=0}^{R} (-1)^{i} \binom{N-R+i-1}{i}$$

$$\times \sum_{\substack{\nu \subseteq \{1,\cdots,N\} \\ |\nu|=R-i,u\subseteq\nu}} \sum_{\mathbf{k}_{|\nu|} \in P^{(n)}} w^{(\mathbf{k}_{|\nu|})} y(\mathbf{x}_{\nu}^{(\mathbf{k}_{|\nu|})}, \mathbf{c}_{-\nu}) \psi_{u\mathbf{j}_{|u|}}(\mathbf{x}_{u}^{(\mathbf{k}_{|u|})}), \quad (68)$$

where $\mathbf{x}_{v}^{(\mathbf{k}_{|v|})} = \{x_{i_1}^{(k_1)}, \cdots, x_{i_{|v|}}^{(k_{|v|})}\}$ and $w^{(\mathbf{k}_{|v|})} = \prod_{p=1}^{p=|v|} w_{i_p}^{(k_p)}$ is the product of integration weights generated by the variables indexed by the elements of v. For independent coordinates of \mathbf{X} , as assumed here, a univariate Gauss quadrature rule is commonly used, where the integration points and associated weights depend on the probability distribution of X_i . They are readily available, for example, the Gauss-Hermite or Gauss-Legendre quadrature rule, when X_i follows Gaussian or uniform distribution. An n-point Gauss quadrature rule exactly integrates a polynomial with a total degree of at most 2n-1.

The S-variate, mth-order PDD approximation requires evaluations of $\sum_{k=0}^{k=S} \binom{N}{k} m^k$ expansion coefficients, including $y_{\emptyset}(\mathbf{d})$. If these coefficients are estimated by dimension-reduction integration with R = S < N and, therefore, involve at most an S-dimensional tensor product of an n-point univariate quadrature rule depending on m, then the total cost for the S-variate, mth-order approximation entails a maximum of $\sum_{k=0}^{k=S} \binom{N}{k} n^k(m)$ function evaluations. If the integration points include a common point in each coordinate — a special case of symmetric input probability density functions and odd values of n — the number of function evaluations reduces to $\sum_{k=0}^{k=S} \binom{N}{k} (n(m)-1)^k$. Nonetheless, the computational complexity of the S-variate PDD approximation is an Sth-order polynomial with respect

to the number of random variables or integration points. Therefore, PDD with dimension-reduction integration of the expansion coefficients alleviates the curse of dimensionality to an extent determined by S.

5.2. Quasi Monte Carlo Simulation

Employing the quasi MCS method for the estimation of the PDD expansion coefficients, which are high-dimensional integrals defined in Equations (2) and (8), again comprises three simple steps: (1) generate a low-discrepancy point set $\mathcal{P}_L := \{\mathbf{u}^{(k)} \in [0,1]^N, \ k=1,\cdots,L\}$ of size $L \in \mathbb{N}$; (2) map each sample from \mathcal{P}_L to the sample $\mathbf{x}^{(k)} \in \mathbb{R}^N$ following the probability measure of the random input \mathbf{X} ; and (3) approximate the coefficients by

$$y_{\emptyset} \cong \frac{1}{L} \sum_{k=1}^{L} y\left(\mathbf{x}^{(k)}\right),\tag{69}$$

$$C_{u\mathbf{j}_{|u|}} \cong \frac{1}{L} \sum_{k=1}^{L} y\left(\mathbf{x}^{(k)}\right) \psi_{u\mathbf{j}_{|u|}}\left(\mathbf{x}_{u}^{(k)}\right). \tag{70}$$

6. Numerical Examples

Two numerical examples are presented to illustrate the hybrid PDD method developed in calculating the second-moment statistics and tail probability distributions of random mathematical functions and random eigensolutions of a simple stochastic dynamical system. Classical Legendre polynomials were used to define the orthonormal polynomials in Example 1, and all PDD expansion coefficients and the hybrid model parameter were determined analytically. In Example 2 all original random variables were transformed into standard Gaussian random variables, facilitating the use of classical Hermite orthonormal polynomials as bases. The expansion coefficients in Example 2 were calculated using dimension-reduction integration (R = 1)involving the five-point univariate Gauss-Hermite quadrature rule. The hybrid model parameter was estimated by quasi MCS using Sobol's low-discrepancy sequence of 100 and 500 points and Equation (54). The sample size for the embedded MCS in Example 2 is 10^6 .

6.1. Polynomial function

Consider the polynomial function

$$y(\mathbf{X}) = \left[\frac{2}{N} \sum_{i=1}^{N} X_i\right]^q,$$

where N = 5, X_i , i = 1, ..., N, are independent and identical random variables, each following the standard uniform distribution over [0, 1], and $q \in \mathbb{N}$ is an exponent. The function $y(\mathbf{X})$ has a purely additive structure when q = 1, but as the value of q increases, the function $y(\mathbf{X})$ evolves from strongly additive to strongly multiplicative. The objective of this example is to compare univariate additive PDD, univariate factorized PDD,

and univariate hybrid PDD approximations in calculating the variance of $y(\mathbf{X})$ for q = 2, 3, 4, 5, 6, 7, 8.

Since y is a multivariate polynomial of degree q, the truncation parameter m for a PDD approximation, whether additive, factorized, or hybrid, was set equal to q. Figure 1 shows how the hybrid model parameter $\alpha_{1,m}$ varies with respect to q, where $\tilde{\sigma}_{1,m}^2$, $\hat{\sigma}_{1,m}^2$, and the expectation in Equation (46) of $\alpha_{1,m}$ are calculated exactly. The parameter $\alpha_{1,m}$ is relatively close to one when q=2, and decreases monotonically as q increases, indicating the diminishing additive structure of the function y. When q=8, $\alpha_{1,m}$ is relatively close to zero, that is, y is dominantly multiplicative.

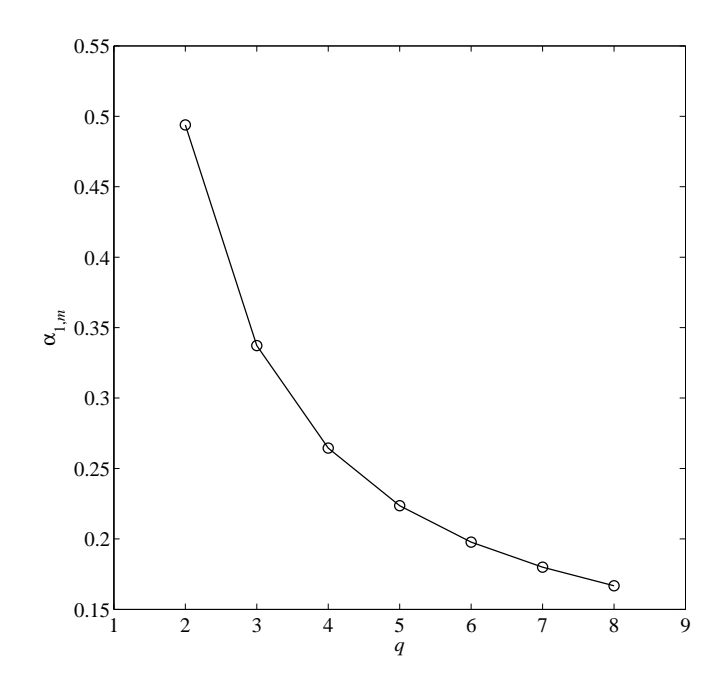


Figure 1: Variation of $\alpha_{1,m}$ with respect to q (Example 1).

Figure 2 presents the relative errors, defined as the ratio of the absolute difference between the exact and approximate variances of y(X) to the exact variance, committed by the univariate additive PDD, univariate factorized PDD, and univariate hybrid PDD methods. The second-moment properties of $y(\mathbf{X})$, given q, were calculated exactly. The function $y(\mathbf{X})$ is strongly additive when q = 2 or 3; therefore, the univariate additive PDD approximation has lower error than the factorized PDD approximation. But the trend reverses for $4 \le q \le 8$, the range of higher values examined. This is because the function switches from dominantly additive $(q \le 3)$ to dominantly multiplicative (q > 3) as q increases. Nonetheless, for all the values of q considered, the univariate hybrid PDD approximation commits lower errors than either univariate additive PDD or univariate factorized PDD approximation. These results are consistent with the findings of Theorem 3.

6.2. Three-degree-of-freedom, undamped, spring-mass system Consider a three-degree-of-freedom, undamped, spring-mass system, shown in Figure 3, with random mass and random stiff-

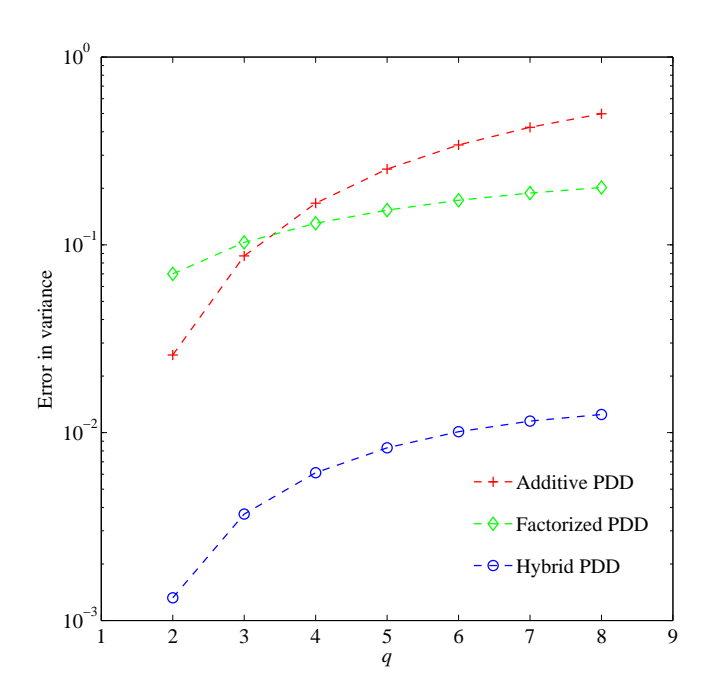


Figure 2: Error in variance calculation from additive PDD, factorized PDD, and hybrid PDD approximations (Example 1).

ness matrices

$$\mathbf{M}(\mathbf{X}) = \begin{bmatrix} M_1(\mathbf{X}) & 0 & 0 \\ 0 & M_2(\mathbf{X}) & 0 \\ 0 & 0 & M_3(\mathbf{X}) \end{bmatrix}$$
(71)

and

$$\mathbf{K}(\mathbf{X}) = \begin{bmatrix} K_{11}(\mathbf{X}) & K_{12}(\mathbf{X}) & K_{13}(\mathbf{X}) \\ & K_{22}(\mathbf{X}) & K_{23}(\mathbf{X}) \\ (\text{sym.}) & K_{33}(\mathbf{X}) \end{bmatrix},$$
(72)

respectively, where $K_{11}(\mathbf{X}) = K_1(\mathbf{X}) + K_4(\mathbf{X}) + K_6(\mathbf{X})$, $K_{12}(\mathbf{X}) = -K_4(\mathbf{X})$, $K_{13}(\mathbf{X}) = -K_6(\mathbf{X})$, $K_{22}(\mathbf{X}) = K_4(\mathbf{X}) + K_5(\mathbf{X}) + K_2(\mathbf{X})$, $K_{23}(\mathbf{X}) = -K_5(\mathbf{X})$, and $K_{33}(\mathbf{X}) = K_5(\mathbf{X}) + K_3(\mathbf{X}) + K_6(\mathbf{X})$; the masses $M_i(\mathbf{X}) = \mu_i X_i$; i = 1, 2, 3 with $\mu_i = 1.0$ kg; i = 1, 2, 3, and spring stiffnesses $K_i(\mathbf{X}) = \mu_{i+3} X_{i+3}$; $i = 1, \cdots, 6$ with $\mu_{i+3} = 1.0$ N/m; $i = 1, \cdots, 5$ and $\mu_9 = 3.0$ N/m. The input $\mathbf{X} = \{X_1, \cdots, X_9\}^T \in \mathbb{R}^9$ is an independent lognormal random vector with mean $\mu_{\mathbf{X}} = \mathbf{1} \in \mathbb{R}^9$ and covariance matrix $\mathbf{\Sigma}_{\mathbf{X}} = \nu^2 \mathbf{I} \in \mathbb{R}^{9 \times 9}$ with coefficient of variation $\nu = 0.3$.

The primary objective of this example is to demonstrate the high accuracy of univariate hybrid PDD approximation in calculating the cumulative distribution functions of the three eigenvalues of the three-degree-of-freedom system. The secondary, although significant, objective of this example is to show that the quasi MCS method, with a relatively small sample size for calculating the model parameter of univariate hybrid PDD approximation, is capable of delivering results comparable to those obtained from the expensive bivariate additive PDD approximation.

The probability distributions of three eigenvalues of the three-degree-of-freedom system were calculated using the

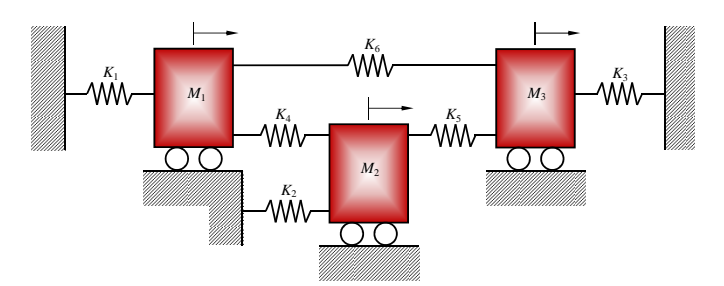


Figure 3: A three-degree-of-freedom, undamped, spring-mass system (Example 2)

benchmark solution of 106 crude MCS method, and five different fourth-order (m = 4) PDD methods: (1) univariate additive PDD, (2) bivariate additive PDD, (3) univariate factorized PDD, (4) univariate hybrid PDD with $\alpha_{1.4}$ estimated using 100 quasi MCS samples, and (5) univariate hybrid PDD with $\alpha_{1.4}$ estimated using 500 quasi MCS samples. Figure 4 presents the marginal probability distributions $F_i(\lambda_i) := P[\Lambda_i \leq \lambda_i]$ of three eigenvalues λ_i , i = 1, 2, 3, where all the PDD solutions were obtained from the embedded MCS; the parenthetical values reflect the total number of function evaluations required by the respective methods. The plots are made over a semi-logarithmic scale to delineate the distributions in the tail regions. For all three eigenvalues, the probability distributions obtained from the univariate additive PDD method is far from the crude MCS results, divulging the clear inadequacy of the univariate additive PDD approximation in calculating tail probabilities. The univariate factorized PDD method performs relatively better than its additive counterpart, indicating the dominantly multiplicative structure of the functions: however, it still leaves much room for improvement compared with the benchmark crude MCS results. The univariate hybrid PDD method requires additional computational effort owing to quasi MCS for estimating $\alpha_{1.4}$ in Equation (54), but the improved results obtained clearly justify the additional cost. To put the results of the univariate hybrid PDD method in perspective, the results from the bivariate (S = 2) additive PDD method, also obtained, show dramatic improvement over the univariate additive PDD method, as expected. However, the bivariate additive PDD method also leads to a significantly larger number of function evaluations compared with the univariate hybrid PDD with quasi MCS (100 samples). Therefore, a hybrid PDD approximation is desirable, where only univariate truncations are feasible, but not necessarily rendering adequate accuracy in stochastic solutions by either additive or factorized PDD approximation alone.

7. Application: A Pickup Truck

This section illustrates the effectiveness of the proposed hybrid PDD method in solving a large-scale practical engineering problem. The application involves predicting the probabilistic characteristics of sound pressure levels inside the cabin of a pickup truck. The acoustics, measured through sound pressure levels, inside a vehicle are widely considered a prominent

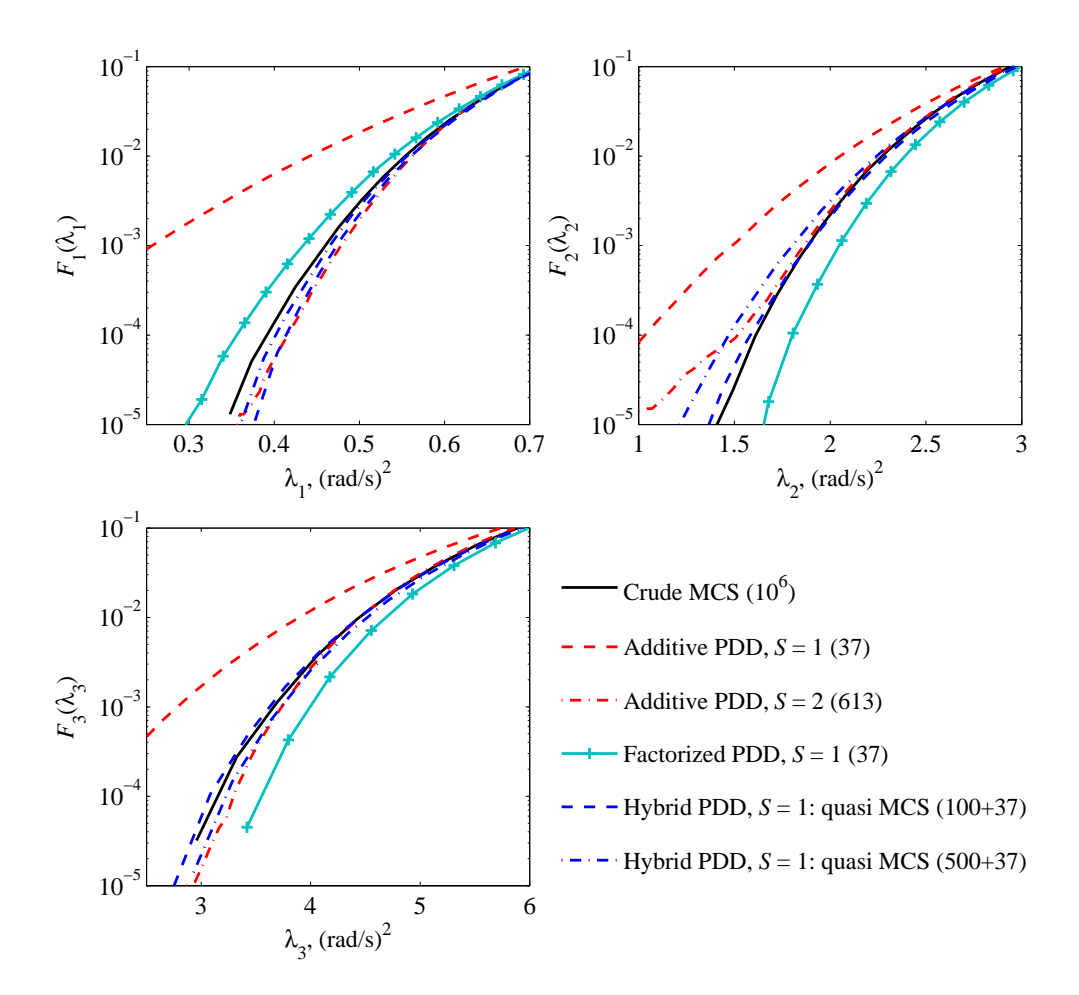


Figure 4: Tail probabilities of three eigenvalues of the three-degree-of-freedom, undamped, spring-mass system by various PDD approximations and crude MCS

parameter revealing the overall quality and build of the vehicle. A coupled acoustic-structural analysis is therefore critically important in the automotive industry as it paves the way towards designing vehicles for ride comfort and quietness. Figure 5(a) presents a computer-aided design (CAD) cabin-air-chassis model of a pickup truck [22]. A finite-element analysis (FEA) mesh of the model, comprising 43,663 structural elements used to model the cabin and the chassis and 12,171 acoustic elements used to model the air interior, with a total of 207,994 degrees of freedom, is displayed in Figure 5(b). Figure 6(a) depicts the cabin model without air mesh and doors to show the space occupied by the air mesh, and Figure 6(b) displays the air mesh that fills the cabin interior. A tie constraint was employed to connect the air mesh to the structural parts inside the cabin surface or onto the seat surface.

Portrayed in Figure 5(a), the CAD model contains 24 distinct materials, with 22 structural materials and two non-structural materials representing the air inside the cabin and the carpet on the cabin floor. Twenty-one of the structural materials were modeled as shell elements, and the remaining material as beam elements defining the circular beam used for headrest mounting. The Young's moduli of 22 structural materials are random variables. The mass densities of the 21 materials modeled as shell elements are also random variables. Apart from the struc-

tural material properties, the bulk modulus and mass density of the air inside the cabin are also random variables. Finally, the proportionality factor between the pressure and velocity of the carpet surface in the normal direction is also a random variable. This proportionality constant defines the acoustic admittance of the carpet surface on the cabin floor. In aggregate, there exist 46 random variables $X_i = 1, ..., 46$, as follows: X_1 to $X_{22} =$ Young's moduli of materials 1 to 22; X_{23} to X_{43} = mass densities of materials 1 to 21; X_{44} = bulk modulus of air inside the cabin; X_{45} = mass density of air inside the cabin; and X_{46} = acoustic admittance of the carpet surface on the cabin floor. All 46 random variables are independent and uniformly distributed with the coefficient of variation equal to 0.2. Table 1 presents the material and part names, and the means of random variables corresponding to the 22 structural materials, $\mu_i := \mathbb{E}[X_i]$, $i = 1, \dots, 43$. The means of the bulk modulus and mass density of air inside the cabin are $\mu_{44} = 0.139$ GPa and $\mu_{45} = 1.2 \times 10^{-12}$ kg/mm³. The mean of the acoustic admittance of the carpet surface on the cabin floor is $\mu_{46} = 0.5 \times 10^6 \text{ mm}^2 \text{s/kg}$. All structural materials, except materials 8, 9, and 10, have a deterministic Rayleigh stiffness proportional damping defined by the parameter $\beta_R = 0.4 \times 10^{-6}$ s. For a given value of β_R , the damping fraction ξ_i for a mode i with natural frequency ω_i is given by the formula $\xi_i = \beta_R \omega_i / 2$. The value of β_R chosen in

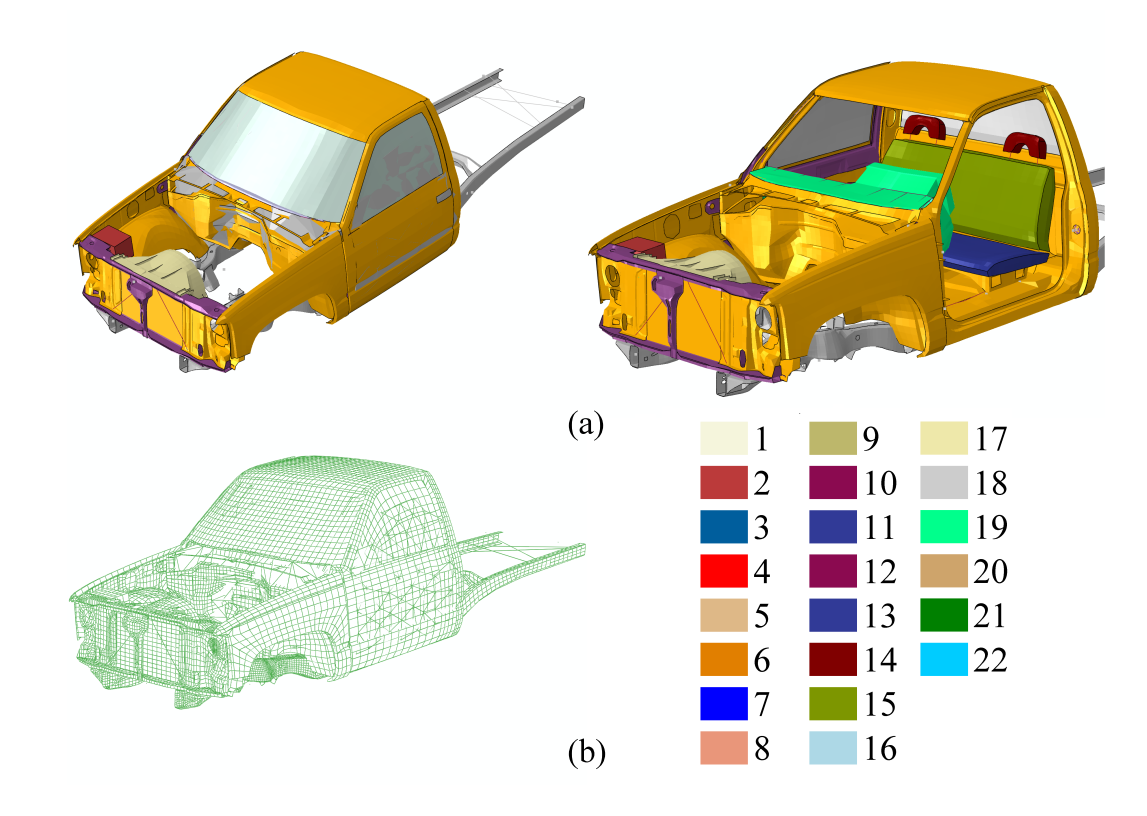


Figure 5: Cabin-air-chassis model of pickup truck: (a) a CAD model, (b) an FEA mesh

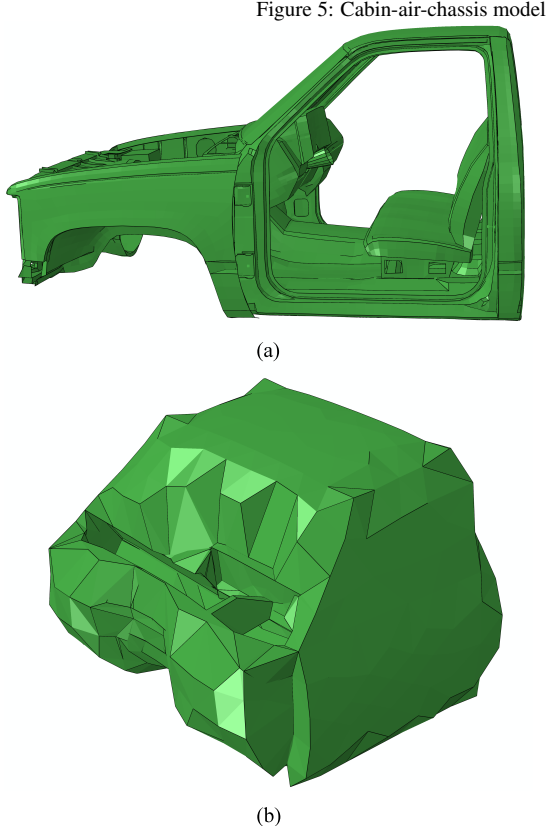


Figure 6: Cabin of pickup truck and air mesh. (a) cabin model of pickup truck with doors removed for clearer illustration; (b) the air mesh inside the cabin

this model is to give approximately 1 percent critical damping for the modes whose natural frequencies are in the middle of the range of excitation, i.e., at about 80 Hz at mean input. The Poisson's ratios of all structural materials are deterministic and are equal to 0.3. The probability distributions of input random variables in this problem were chosen arbitrarily, as the main purpose was to demonstrate the ability of the proposed method in solving large-scale practical engineering problems. Identifying more realistic probability distributions for each material will require additional studies that are beyond the scope of this work.

7.1. Coupled acoustic-structural analysis

A mode-based coupled acoustic-structural analysis consists of two steps: an eigensolution extraction followed by a steady-state dynamic analysis involving sound pressure level calculations. For obtaining eigensolutions, the first 200 eigenfrequencies were extracted. The Lanczos method [23] embedded in Abaqus (Version 6.12) [22] was employed for extracting natural frequencies and mode shapes. For steady-state dynamic analysis, the airborne load originating from engine vibration was modeled as a diffuse field incident wave loading on the bulkhead below the dashboard. In the steady-state dynamic analysis, the sound pressure level at a location in the vicinity of the driver's ear was calculated. The location of the driver's ear was defined through a node in the air mesh inside the cabin, in accordance with the specifications of location for measurement of noise inside motor vehicles defined in International Standard

Table 1: Material, part name, and mean values of the random input variables for structural materials in pickup truck

Material	Material name	Young's modulus	Mass density	Part name
		GPa	kg/m^3	
1	Steel	210	7890	Rail (chassis), bed, cabin, fenders, engine oil box.
2	Steel	210	7890	Wheel housings, rear rim, steering support, battery
2	Steel	210	1090	tray, seat track.
3	Steel	210	7890	Radiator mounting, radiator outer, fan center, fuel
				tank.
4	Steel	210	7890	Engine mountings, fender mountings, hood, doors,
				cabin hinges.
5	Plastic	2.8	1200	Fan cover.
6	Glass	76	2500	Windows, windshield.
7	Plastic	3.4	1100	Radiator side block.
8	Steel	210	7890	Rear axle, drive shaft, steering, steering column,
				gearbox CV joint, brakes.
9	Steel	210	20900	Brake assembly.
10	Steel	210	6910	Brake assembly.
11	Rubber	250	8060	Tires.
				A-arm mountings, A-arm-rim connectors, A-arm-rail
12	Steel	210	7890	connectors, front rim, bed-rail connector, rail
				connector.
13	Foam	2.0	253	Seat bottom.
14	Foam	2.0	755	Seat top.
15	Foam	2.0	169	Seat headrest.
16	Steel	210	2500	Door lock.
17	Steel	200	7800	Radiator.
18	Rubber-Metal	210	1960	D. (1)
	Composite			Battery.
19	Steel	120	3890	Engine gearbox.
20	Steel	21	1820	Engine front.
21	Steel	210	7890	Headrest connector beams, fan, door lock beams, oil
				pan beams, dashboard support.
22	Steel	210	_(a)	Radiator mounting beams.

⁽a) Not required.

ISO-5128 [24]. The values of the sound pressure level were calculated at 200 evenly spaced points in the excitation frequency range of 35 Hz to 120 Hz. This frequency range corresponds to engine-induced vibrations in the range of 2100-7200 rpm. The governing equations of a coupled acoustic-structural analysis are described in Appendix A.

Due to the uncertainty in material properties, the eigensolutions and sound pressure level values are random functions. The univariate, second-order hybrid PDD approximation was employed to determine their second-moment characteristics and various response probabilities. The associated expansion coefficients of PDD and the hybrid model parameter were estimated by the quasi MCS method with 500 samples. The sample size for the embedded MCS of the PDD approximation is 5000.

7.2. Moments of mode shapes

The univariate, second-order hybrid PDD method was employed to calculate the second-moment statistics of each nodal pressure component of an eigenvector describing the associated mode shape of the air inside the cabin. All input random

variables were transformed into uniform random variables, permitting the use of Legendre orthonormal polynomials as basis functions. The second-moment statistics were calculated from Equations (69) and (53), where the hybrid model parameter was estimated from Equation (55). Based on these statistics, the \mathcal{L}_2 -norms (square root of sum of squares) of the mean and variance of a nodal pressure were calculated. Figures 7(a) and (b) present contour plots of the \mathcal{L}_2 -norms of the mean and variances, respectively, of an arbitrarily selected 35th mode shape, calculated using hybrid PDD approximation. Similar results can be generated for other mode shapes if desired.

7.3. Probabilistic characteristics of sound pressure level

The sound pressure level in decibels (dB) is calculated in the vicinity of the driver's ear as SPL = $20 \log_{10} \left[p / \left(p_{ref} \sqrt{2} \right) \right]$, where p is the pressure in Pa obtained in mode-based steady-dynamic analysis, and $p_{ref} = 2 \times 10^{-5}$ Pa is the *zero* or reference sound pressure, which is considered the threshold of human hearing.

Figure 8 shows various percentiles of sound pressure level in the vicinity of the driver's ear calculated from the univari-

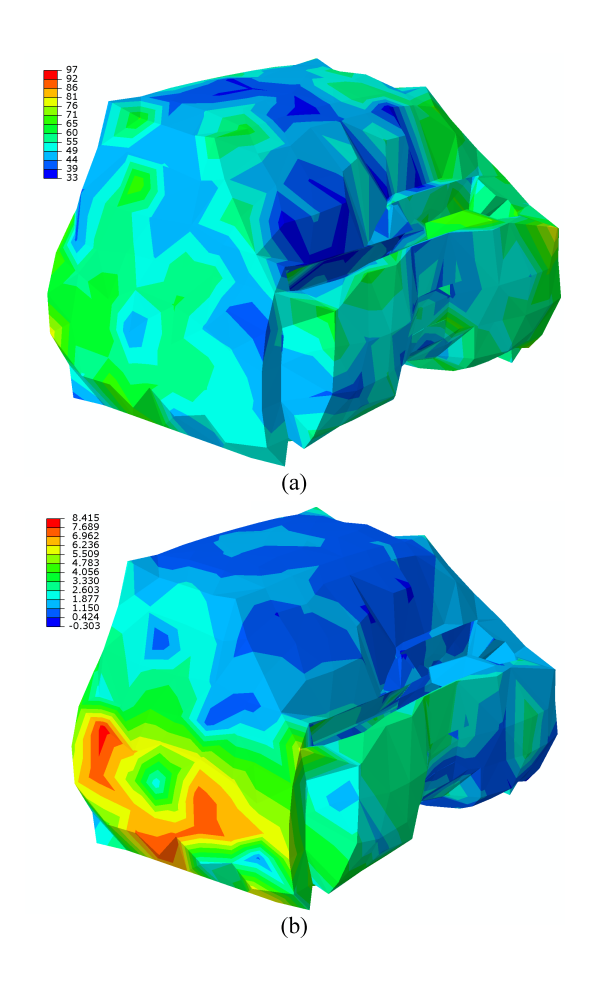


Figure 7: Contour plots of the \mathcal{L}_2 -norms of 35th mode shape of air inside the cabin of a pickup truck by the hybrid PDD approximation: (a) mean, (b) variance

ate, second-order hybrid PDD approximation. The percentiles were calculated from 5000 embedded MCS of the hybrid PDD approximation at 200 evenly spaced points in the excitation frequency range of 35 Hz to 120 Hz. Figure 9 presents the probability density function of the maximum sound pressure level in the excitation frequency range of 35 Hz to 120 Hz, as calculated from 5000 embedded MCS of the hybrid PDD approximation. These results provide vital information pertaining to the acoustic performance of the vehicle operating under several random input parameters. A designer can utilize these valuable results for optimizing the vehicle design to achieve a desired acoustic performance.

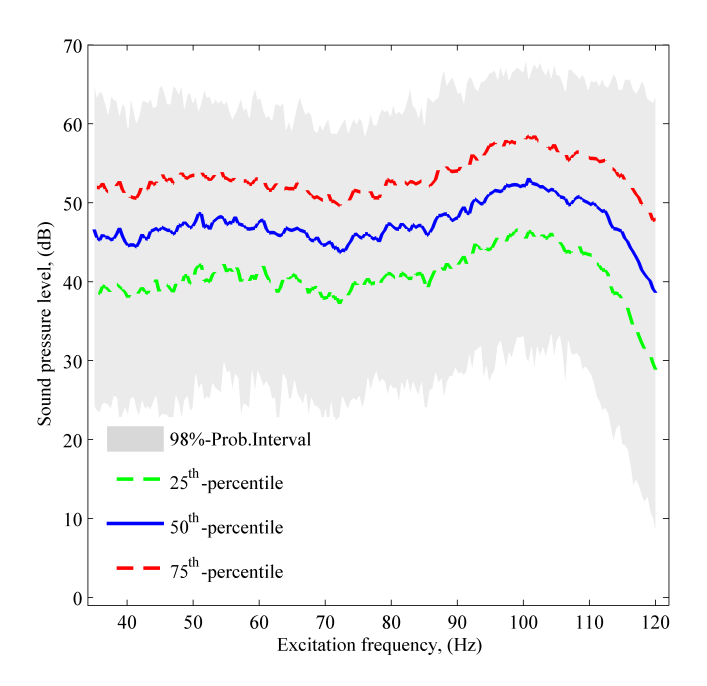


Figure 8: Percentiles of sound pressure levels in the vicinity of the driver's ear in a pickup truck by the hybrid PDD approximation

8. Conclusion

A new hybrid PDD method was developed for uncertainty quantification of high-dimensional complex systems. method is built from a linear combination of an additive and a multiplicative PDD approximation, both obtained from lower-dimensional ANOVA component functions of a general, square-integrable multivariate function. When a stochastic response is not endowed with a specific dimensional hierarchy, the hybrid PDD approximation, optimally blending the additive PDD and multiplicative PDD approximations, is the best choice. A theorem and a corollary proven herein give analytical expressions for the model parameters that form the linear combinations of additive PDD and multiplicative PDD approximations, resulting in the hybrid PDD method. Using properties of orthonormal polynomials, explicit formulae were derived for calculating the response statistics by the univariate hybrid PDD approximation.

The univariate truncation of the hybrid PDD was employed to calculate the second-moment properties and tail probability

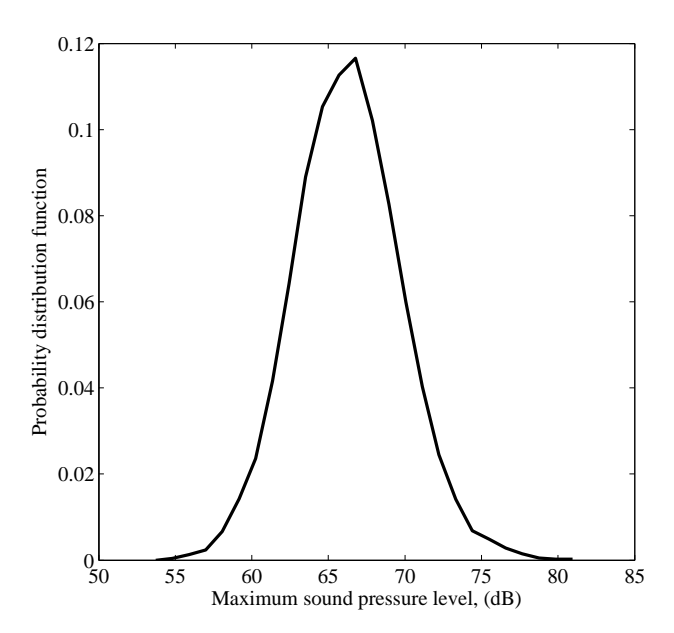


Figure 9: Probability density function of the maximum sound pressure level in excitation frequency range of 35 Hz to 120 Hz by the hybrid PDD approximation

distribution in two numerical problems, where the output functions are either simple mathematical functions or eigenvalues of a simple linear oscillator. For a function with a mixed additive and multiplicative structure, the univariate hybrid PDD approximation commits remarkably lower errors in calculating the variance compared with both univariate additive and multiplicative PDD approximations. The univariate hybrid PDD approximation is also more accurate than either the univariate additive or multiplicative PDD methods, and is more efficient than the bivariate additive PDD method in determining the tail probabilistic characteristics of eigenvalues of the dynamic system examined. Therefore, the univariate truncation of the hybrid PDD is ideally suited to solving stochastic problems that may otherwise mandate expensive bivariate or higher-variate additive or multiplicative PDD approximations. Finally, a successful evaluation of random eigensolutions of a pickup truck, subjected to 46 input random variables, involving coupled acoustic-structure analysis demonstrates the ability of the new method in solving large-scale practical engineering problems.

Appendix A. Governing Equations for Coupled Acoustic-Structural Analysis

A coupled acoustic-structural analysis involves solution of the acoustic variational equation

$$\int_{V_{f}} \left[\delta p \left(\frac{1}{K_{f}} \ddot{p} + \frac{\gamma}{\rho_{f} K_{f}} \dot{p} \right) + \frac{1}{\rho_{f}} \frac{\partial \delta p}{\partial \mathbf{x}} \cdot \frac{\partial p}{\partial \mathbf{x}} \right] dV - \int_{S_{ft}} \delta p T_{0} dS
+ \int_{S_{fr}} \delta p \left(\frac{\gamma}{\rho_{f} c_{1}} p + \left(\frac{\gamma}{\rho_{f} k_{1}} + \frac{1}{c_{1}} \right) \dot{p} + \frac{1}{k_{1}} \ddot{p} \right) dS
+ \int_{S_{ft}} \delta p \left(\frac{1}{c_{1}} \dot{p} + \frac{1}{a_{1}} p \right) dS - \int_{S_{fs}} \delta p \mathbf{n}^{-} \cdot \ddot{\mathbf{u}}^{m} dS
+ \int_{S_{frs}} \delta p \left(\frac{\gamma}{\rho_{f} c_{1}} p + \left(\frac{\gamma}{\rho_{f} k_{1}} + \frac{1}{c_{1}} \right) \dot{p} + \frac{1}{k_{1}} \ddot{p} - \mathbf{n}^{-} \cdot \ddot{\mathbf{u}}^{m} \right) dS
= 0,$$
(A.1)

and the structural virtual work equation

$$\int_{V} \delta \epsilon : \sigma dV + \int_{V} \alpha_{c} \rho \delta \mathbf{u}^{m} \cdot \dot{\mathbf{u}}^{m} dV + \int_{V} \rho \delta \mathbf{u}^{m} \cdot \ddot{\mathbf{u}}^{m} dV + \int_{S} \rho \delta \mathbf{u}^{m} \cdot \mathbf{n} dS - \int_{S} \delta \mathbf{u}^{m} \cdot \mathbf{t} dS = 0$$
(A.2)

simultaneously for the structural displacement \mathbf{u}^m and the acoustic "displacement" or pressure p. In Equations (A.1) and (A.2), K_f is the bulk modulus of the fluid acoustic medium of volume V_f ; γ is the volumetric drag, or force per unit volume per velocity, in the fluid; ρ_f is the mass density of the fluid; δp is the pressure variation in the fluid; **x** is spatial position of the fluid particle; T_0 is the prescribed boundary traction over S_{ft} , the acoustic boundary subregion where the normal derivative of the acoustic medium is prescribed; $1/c_1$ and $1/k_1$ are the proportionality coefficients between the pressure and velocity, and the pressure and displacement, respectively, normal to the surface of the fluid; S_{fr} is the reactive acoustic boundary subregion; S_{fi} is the radiating acoustic boundary subregion; S_{frs} is the acoustic boundary subregions where the displacements are linearly coupled but not necessarily identically equal due to the presence of a compliant or reactive intervening layer; n⁻ is the outward normal to the structure; σ is the stress at a point on the structure; $\delta \epsilon$ is the strain variation in the structure; α_c is the mass proportional damping factor; ρ is the mass density of the structure; and \mathbf{t} is the surface traction applied over the surface S_t of the structure. Further details are available elsewhere [25].

References

- S. Rahman, A polynomial dimensional decomposition for stochastic computing, International Journal for Numerical Methods in Engineering 76 (2008) 2091–2116.
- S. Rahman, Extended polynomial dimensional decomposition for arbitrary probability distributions, Journal of Engineering Mechanics 135 (2009) 1439–1451.
- [3] S. Rahman, V. Yadav, Orthogonal polynomial expansions for solving random eigenvalue problems, International Journal for Uncertainty Quantification 1 (2011) 163–187.
- [4] V. Yadav, S. Rahman, Adaptive-sparse polynomial dimensional decomposition methods for high-dimensional stochastic computing, Computer Methods in Applied Mechanics and Engineering 274 (2014) 56 83.

- [5] R. Bellman, Dynamic Programming, Princeton University Press: Princeton, NJ, 1957.
- [6] W. J. Morokoff, R. E. Caflisch, Quasi-monte carlo integration, Journal of Computational Physics 122 (1995) 218–230.
- [7] V. Yadav, S. Rahman, Uncertainty quantification of high-dimensional complex systems by multiplicative polynomial dimensional decompositions, International Journal for Numerical Methods in Engineering 94 (2013) 221–247.
- [8] I. M. Sobol, Theorems and examples on high dimensional model representation, Reliability Engineering & System Safety 79 (2003) 187 193.
- [9] F. Y. Kuo, I. H. Sloan, G. W. Wasilkowski, H. Wozniakowski, On decompositions of multivariate functions, Mathematics of Computation 79 (2011) 953–966.
- [10] S. Rahman, Approximation errors in truncated dimensional decompositions, Accepted in Mathematics of Computation (2014).
- [11] S. Rahman, Statistical moments of polynomial dimensional decomposition, Journal of Engineering Mechanics 136 (2010) 923–927.
- [12] M. A. Tunga, M. Demiralp, A factorized high dimensional model representation on the nodes of a finite hyperprismatic regular grid, Applied Mathematics and Computation 164 (2005) 865–883.
- [13] S. Rahman, Uncertainty quantification by alternative decompositions of multivariate functions, SIAM Journal on Scientific Computing 35 (2013) A3024–A3051.
- [14] H. Niederreiter, Random Number Generation and Quasi-Monte Carlo Methods, CBMS-NSF Regional Conference Series in Applied Mathematics, Society for Industrial and Applied Mathematics, 1992. URL: http://books.google.com/books?id=pca2tPZozXcC.
- [15] J. Halton, On the efficiency of certain quasi-random sequences of points in evaluating multi-dimensional integrals, Numerische Mathematik 2 (1960) 84–90.
- [16] H. Faure, Discrépances de suites associées à un système de numération (en dimension un), Bulletin de la Société Mathématique de France 109 (1981) 143–182.
- [17] I. M. Sobol, On the distribution of points in a cube and the approximate evaluation of integrals, U.S.S.R. Comput. Math. Math. Phys. 7 (1967) 86–112.
- [18] I. Sloan, S. Joe, Lattice Methods for Multiple Integration, Oxford science publications, Clarendon Press, 1994. URL: http://books.google.com/books?id=9twIWULueasC.
- [19] X. Wang, Improving the rejection sampling method in quasi-monte carlo methods, Journal of Computational and Applied Mathematics 114 (2000) 231 – 246.
- [20] H. Xu, S. Rahman, A generalized dimension-reduction method for multidimensional integration in stochastic mechanics, International Journal for Numerical Methods in Engineering 61 (2004) 1992–2019.
- [21] H. Xu, S. Rahman, Decomposition methods for structural reliability analysis, Probabilistic Engineering Mechanics 20 (2005) 239 – 250.
- [22] ABAQUS Standard, Version 6.12, Dassault Systems Simulia Corp, 2012.
- [23] J. K. Cullum, R. A. Willoughby, Lanczos Algorithms for Large Symmetric Eigenvalue Computations: Theory, Classics in applied mathematics, Society for Industrial and Applied Mathematics, 2002.
- [24] ISO-5128, Acoustics Measurement of noise inside motor vehicles, International Organization for Standardization, Geneva, Switzerland, 1980.
- [25] P. Morse, K. Ingard, Theoretical Acoustics, McGraw-Hill, 1968.